Biogeochemical drivers of interspecies electron transfer between iron reducers and methanogens

by

Javil Hansen

B.S., Kansas State University, 2018

A THESIS

submitted in partial fulfillment of the requirements for the degree

MASTER OF SCIENCE

Department of Geology
College of Arts and Sciences

KANSAS STATE UNIVERSITY
Manhattan, Kansas

2021

Approved by:

Major Professor
Matthew F. Kirk

Copyright

Abstract

Iron reduction and methanogenesis help drive the carbon cycle and in doing so influence greenhouse gas emissions and water quality. Microorganisms that drive the reactions can compete for energy sources or engage in syntropy via interspecies electron transfer (IET), but it remains unclear how environments influence which of these interactions occur. This study uses culturing experiments containing *Geobacter metallireducens* and *Methanosarcina barkeri* to better understand how interactions between an iron reducer and a methanogen, respectively, change with conditions. We examined interactions in iron reduction and methanogenesis in batch reactors with varying ferric iron mineralogy (none, ferrihydrite, lepidocrocite, goethite, and hematite) and acetate concentration (3 and 30 mM) and in semi-continuous cultures with varying acetate (3 and 30 mM) and bicarbonate (24 and 48 mM) concentrations but no ferric iron mineral. Results of the batch experiments show that amounts of methanogenesis varied considerably with ferric iron mineralogy and acetate supply. Average CH_4 generation was higher in cultures with 30 mM acetate than those with 3 mM acetate and decreased in order of hematite >> no ferric mineral ~ goethite > ferrihydrite > lepidocrocite. By comparison, the amount of iron reduction varied relatively little with acetate concentration and was lowest in cultures with hematite. In the semi-continuous cultures, CH_4 concentrations increased over time and reached the highest values in cultures with the 30 mM acetate and 24 mM bicarbonate. Carbon stable isotope compositions ($\delta^{13}C$) of CO_2 and CH_4 from both culturing experiments suggest that differences in CH_4 generation between cultures may in part reflect variation in the pathway of methanogenesis. Carbon isotopic compositions from cultures with hematite were consistent with CH_4 generation via acetoclastic methanogenesis. However, results from other cultures are more

indicative of methanogenesis by CO_2 reduction. No hydrogen sources were available in the reactor to drive CO_2 reduction. Therefore, the result suggests that IET fueled much of the methanogenesis in the cultures. Taken together, our results indicate that the occurrence of IET can be influenced by ferric iron mineralogy and concentration of acetate. Impacts of IET on carbon isotope systematics in methanogenic systems require more attention. In particular, we need a better understanding of differences in the $\delta^{13}C$ of CO_2 and CH_4 evolve as substrate consumption proceeds.

Table of Contents

List of Figures

List of Tables

Chapter 1 - Introduction

Microbial iron reduction and methanogenesis help drive organic matter oxidation in anoxic environments and in doing so, impact water quality and greenhouse gas emissions (Emerson et al., 2012; Melton et al., 2014; Thauer et al, 2008). Iron reduction traps carbon by generating carbonate alkalinity but degrades water quality by increasing concentrations of iron and trace elements (e.g., arsenic) (Kirk et al, 2013). Methanogenesis produces CH_4, which contributes significantly to energy resources (Milkov, 2011) but also strengthens the greenhouse effect by escaping to the atmosphere (Forster et al., 2017; Kirschke et al., 2013). Thus, impacts of iron reduction and methanogenesis can be beneficial or harmful, depending on the setting and proportions of the reactions relative to one another. By learning more about environmental controls on interactions between the microbes that catalyze the reactions, we will be better able to predict and manage these impacts.

Iron reducers and methanogens were previously thought to occupy separate zones defined by competition (Lovley and Goodwin, 1988; Achtnich, et al., 1995). This conceptual model followed the thermodynamic ladder in geomicrobiology, where anaerobic microorganisms arrange themselves into zones based on the quantity of energy they can capture from the environment (Bethke et al., 2011). According to the model, iron reduction is assumed to have a thermodynamic advantage over methanogenesis and thus, the microbial community would deplete ferric iron from an environment before significant methanogenesis occurred. However, the natural world is rarely at standard state, so this thermodynamic order cannot be assumed to always hold true. Moreover, interactions between microbial reaction do not depend entirely on thermodynamic controls. Kinetic controls are also play an important role (Bethke et al., 2008, 2011).

Results from several studies underscore shortcoming of the traditional paradigm. Several studies have found evidence that iron reduction and methanogenesis can occur concurrently (Flynn et al., 2013; Herndon et al., 2015; Jakobsen and Postma, 1999; Küsel et al., 2018; Metje and Frenzel, 2007; Paul et al., 2006; Reiche et al., 2008). Moreover, interactions between iron reducers and methanogens are not only restricted to competition. These groups can also interact syntrophically via interspecies electron transfer (IET) (Rotaru et al., 2014a, 2014b;). During IET, iron reducers consume electron donor(s) and, rather than transfer the electrons to a source of ferric iron, they transfer them to methanogens, who use them to reduce CO_2 and generate CH_4 (Lovely, 2017). The interaction is said to be direct interspecies electron transfer (DIET) if the electrons are passed via direct connections rather than soluble electron shuttles.

Recent research suggests that pH and ferric iron mineralogy have the potential to influence how iron reducers and methanogens interact. Marquart et al. (2019) found evidence that pH may influence interactions by affecting the energy yield of iron reduction. In their experiments, as pH increased, methanogenesis increased relative to iron reduction and yet the relative abundance of iron reducing populations held steady. The authors suggested that they increasingly participated in methanogenesis via IET as pH increased and the energy yield of iron reduction decreased. Ferric iron mineralogy has the potential to influence interactions by providing pathways for electron transfer (Liu et al., 2012).

These studies advance our understanding of controls on interactions of iron reduction and methanogenesis and yet many questions remain unresolved. Will we see greater occurrences of IET in systems with more stable ferric iron minerals? As iron mineral stability increases, the energy yield of iron reduction decreases (Fig. 1), potentially encouraging iron reducers to cooperate with methanogens rather than compete with them. How does variation in the

availability of electron donors affect interactions? Iron reducer enzymes have a higher affinity than methanogens for competitive substrates such as acetate and dihydrogen (Bethke et al., 2008). However, their ability to exploit this competitive advantage would decrease if electron donors are supplied at a rate that is high relative to the availability of ferric iron. Lastly, does the concentration of bicarbonate influence interactions? Bicarbonate is a product of iron reduction and acetoclastic methanogenesis, and thus decreases the energy yield of both reactions as its concentration increases. However, dissolved inorganic carbon species such as bicarbonate are reactants in methanogenesis via IET. Thus, we reason that increasing levels of bicarbonate have the potential to promote IET.

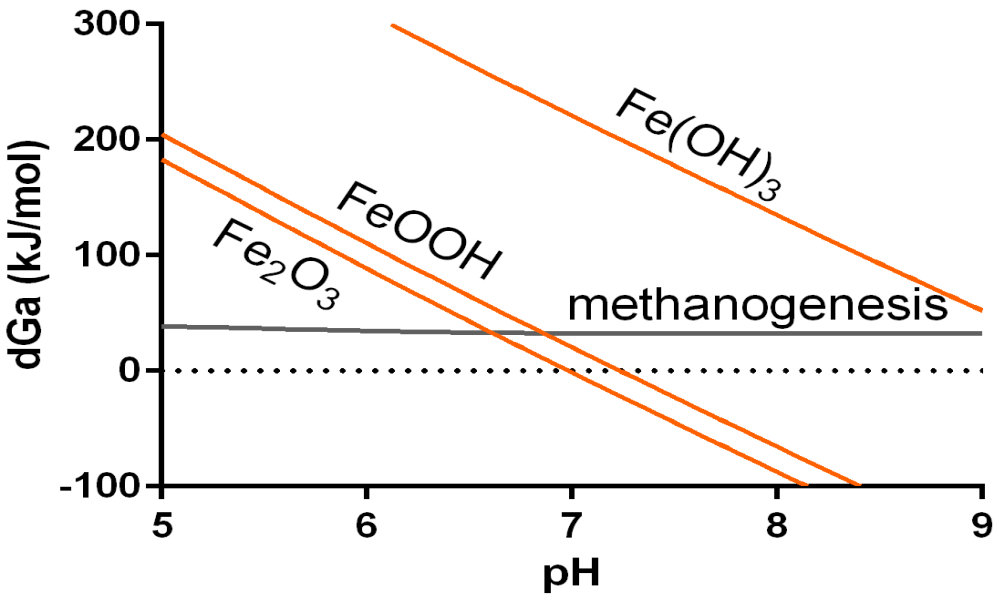

Figure 1 Variation with pH in the energy available (ΔGa) to acetoclastic methanogenesis and ferric iron (Fe(III)) reduction. Sources of ferric iron considered are hematite (α-Fe_2O_3), goethite (α-FeOOH), magnetite (Fe_3O_4), and ferrihydrite (~$Fe(OH)_3$). All reactions were written in terms of the oxidation of one mole of acetate. Values of ΔGa were calculated from chemical activities generated from a sliding pH speciation model for a nominal geochemical environment at 25°C, following Bethke et al. (2011).

We examined these questions using culturing experiments containing *Geobacter metallireducens* and *Methanosarcina barkeri*, an iron reducer and methanogen, respectively, that are known to be capable of IET (Rotaru et al., 2014a). We used a batch experiment to test variation in ferric iron mineralogy and electron donor concentration and we used a semi-continuous experiment to examine variation in interactions over time in systems with variable concentrations of acetate and bicarbonate. In addition, we carried out some control experiments containing only *M. barkeri* to evaluate how electron donor source affected the stable isotopes of carbon in CH_4 and CO_2, which we use as a tracer for the pathway of methanogenesis in our cultures.

Chapter 2 - Methods

2.1 Aqueous Media

We based the aqueous media for this experiment from a modified Rotaru et al. 2014 media based on personal correspondence with Amelia Rotaru. The base medium consisted of 2MΩ deionized water enriched with 0.35 g/L K_2HPO_4, 0.23 g/L KH_2PO_4, 0.5 g/L NH_4Cl, 2.3377 g/L NaCl, 1 ml of 0.516% $FeSO_4$, and 1 ml/L of ATTC trace mineral supplement. We added 90 ml of base medium into 160 ml serum bottles. Each bottle was sparged for 30 minutes with an 80:20 mix of N_2:CO_2 gas to remove trace oxygen and set the pH. We then sealed, crimped, sterilized by autoclaving at 121° C for 30 minutes, and allowed the bioreactors to cool. We placed the bioreactor bottles in an anaerobic chamber to aseptically add the following additions: 1 ml of filter sterilized vitamin supplement, 2.4 ml of 1M HCO_3^-, 1 ml of 3.66% $MgCl_2$, 1 ml of 1.887% $CaCl_2$, and 1 ml of 12.009 g/l NaS with 17.56 g/l cysteine. We sparged with N_2 gas for 30 minutes the $MgCl_2$, $CaCl_2$, acetate, and NaS with cysteine solutions. We sparged the HCO_3^- for 30 minutes with a 80% N_2 and 20% CO_2 gas mixture. Prior to addition, we sterilized all additions by autoclaving at 121º C for 30 minutes. We verified the final pH of the media was at the target pH of 7, and adjusted gas concentrations if needed. Final mM concentrations of the aqueous media are shown in Table 1. Acetate and HCO_3^- concentrations are two of the variables used in our experiments, and thus vary in some experiments.

Table 1 – Aqueous media composition

Component	mM
K_2HPO_4	2
KH_2PO_4,	1.69

NH_4Cl	9.35
NaCl	40
$FeSO_4$	.013
HCO_3^-	2.4
Acetate	30
$CaCl_2$	1.70
$MgCl_2$	3.84
NaS	5.22
Cysteine	1.45

2.2 Microbes

Our experiments included *Geobacter metallireducens* (ATTC 53774) as the iron reducer and *Methanosarcina barkeri Schnellen (*ATTC 43241) as the methanogen. We selected these species because previous research demonstrated that they are both capable of interacting through IET. Moreover, both species are capable of consuming acetate, the electron donor provided in our aqueous medium (Rotaru et al., 2014a, 2014b;).

*G. metallireducen*s is an obligate anaerobe, with a reported optimal pH range of 6.7 to 7 (Lovely et al., 1988). *G. metallireducen*s is capable of utilizing a wide range of compounds as an electron donor source, including acetate, benzaldehyde, benzoate, benzylalcohol, butanol, butyrate, p-cresol, ethanol, p-hydroxybenzaldehyde, phydroxybenzoate, p-hydroxybenzylalcohol, isobutyrate, isovalerate, phenol, propionate, propanol, pyruvate, toluene and valerate (Lovely, 1991). However, acetate is expected to be the primary electron donor during iron reduction in aquatic sediments and subsurface environments (Lovely, 1995). *G.*

*metallireducen*s has three pathways to consume acetate as an electron donor, making it well suited to metabolize acetate at low concentrations naturally found in the environment (Akular, et al., 2009).

M. barkeri Schnellen is an obligate anaerobe, with an optimal pH range of between 6.7 and 7.5 (Appels et al., 2008; Gujer and Zehdner, 1983). *M. barkeri* Schnellen has a higher growth rate (doubling times reported in the order of 1.0-1.2 days) and is more tolerant to sudden pH changes (can tolerate sudden pH changes of 0.8-1.0 units) than most methanogens (Conklin et al., 2006; Liu et al., 1985; Shin et al., 2011). *M. barkeri* Schnellen is able to utilize acetate, hydrogen, or methanol as an electron donor source (Thauer et al., 2008).

We grew the inoculum to late exponential/early stationary phase, as determined from lab experiments using ferrous iron and CH_4 concentrations as growth markers. This was approximately one week for *G. metallireducens* and 2 weeks for *M. barkeri.* We used 0.5 ml of *G. metallireducens* culture containing approximately 4.5 million cells/ml, for an initial cell abundance of 22,5000 cells/ml, and 1 ml of *M. barkeri* culture containing approximately 100,000 cells/ml as an inoculum creating an initial abundance of 1,000 cells/ml.

2.3 Ferric Iron Mineral Experiments

We used batch cultures to study effects on ferric iron mineral source on interactions between iron reducers and methanogens. We inoculated the batch bioreactors after setting up the bottles with 100 ml of media as described. We used 3 mM and 30 mM acetate concentrations and amended the bioreactors with 10 mM of goethite, lepidocrocite, hematite, ferrihydrite, or no mineral, for a total of ten conditions. We replicated the conditions in sets of triplicates with one sterile control. We incubated the bioreactors undisturbed, in the dark at 20° C for 42 days.

After the incubation time, we extracted samples for analyses. We measured the pressure of each bioreactor using a gas gauge. We removed 1 ml of gas from the headspace, which we ran through a gas chromatograph to obtain CH_4 concentrations. We removed liquid sample with a sterile syringe and filtered the samples through a 0.45 μm filters. We recorded pH values of the filtered samples immediately using a pH meter. We used the remaining aqueous sample volume for geochemical analyses and cell counts.

2.4 Semi-Continuous Experiments

We used semi-continuous cultures to examine changes over time with variations of HCO_3^- concentrations alongside variations of acetate concentrations. We set up each bioreactor using the same media and methods as described earlier, with the addition of a needle placed into the rubber stopper to allow sampling and feeding of the bioreactors. We tested two variables with the semi-continuous bioreactors: bicarbonate and acetate concentrations. We used 24 mM and 48 mM bicarbonate concentrations and 3 and 30 mM acetate concentration, for a total of four different conditions. We performed each set of bioreactor conditions in triplicate along with one sterile control.

Batch cultures incubated undisturbed, in the dark, at 20° C for seven-day intervals. Every seventh day, we removed the bioreactors for sampling and feeding. Sampling and feeding consisted of withdrawing 20 ml from the bioreactors and replacing with 20 ml of fresh, sterile medium. We sampled the bottles for a total of eight periods of seven days. Every 7 days, we took the pressure in PSI using a sterile syringe took out 1 ml of sample for GC analysis, and replaced with 1 ml of N_2 gas.

2.5 Methanogen Substrate Experiments

To evaluate isotopic signatures of methanogenic pathways, we made four triplicate sets of bioreactor experiments using the base media described earlier supplied with different electron donor sources. We amended the aqueous media of one bioreactor triplicate set with 30 mM acetate concentrations, and one set with 20 mM methanol. We supplied 450 µmol hydrogen to one set by sparging with a gas mixture of 60% N_2, 20% CO_2, and 20% H_2. We included one sterile control using the same conditions for each set of triplicates. We inoculated each bioreactor with 1 ml of *M. barkeri.* We incubated the cultures in the dark, undisturbed at 20° C for 42 days. We removed the cultures, withdrew 1 ml of headspace to obtain CH_4 concentrations using gas chromatography analysis.

2.6 Chemical Analysis

We extracted aqueous and gas samples weekly from semi-continuous experiments and took samples at the end of incubation for ferric iron mineral and methanogen substrate experiments. We used all aqueous samples to measure pH and concentrations of major cations (Na^+, NH_4^+, K^+, Mg^{2+}, and Ca^{2+}) and anions (CH_3COO^-, Cl^-, NO_3^-, Br^-, and PO_4^{2-}). For semi-continuous experiments, we alternated weekly aqueous samples for alkalinity measurements or cell counts. We measured alkalinity and took cell counts at the end of incubation for ferric iron mineral experiments and methanogen substrate experiments. For experiments containing ferric iron, we measured aqueous Fe(II) and total Fe(II) using 0.5 N HCl extractions.

Before performing analysis, we filtered all aqueous samples using syringe filters with 0.45 µm filters. We measured the pH with an Oakton PC300 pH meter. For analysis of anion and cation samples, we used a Dionex ICS-1100 Ion Chromatograph. We calculated alkalinity using Gran alkalinity titrations with 0.02 N sulfuric acid titrant. For CH_4 analysis we used a GOW

MAC series 580 gas chromatograph equipped with a thermal conductivity detector. Before extracting gas samples, we measured the pressure each bioreactor using a low-pressure mechanical gauge.

We obtained aqueous ferrous iron concentrations by adding 1 ml of 0.45 μm filtered, freshly removed bioreactor samples to 2.5 ml of 1g/L ferrozine and 46 mM HEPES reagent. If the samples appeared to be darker than our high standard of 10 mg/L ferrous iron, we diluted the samples with 18 MΩ deionized water. We shook the samples to mix them and recorded the ABS of each sample using a Thermo Scientific Genesys 10S UV-VIS spectrophotometer set at 562 nm (Stookley, 1970; Gibbs 1976). Using linear regression from standards prepared at our lab we recorded ferrous iron concentration and applied the dilution factor to obtain final ferrous iron concentrations.

We obtained total ferrous iron using 0.5 N HCl extractions. We vigorously shook the bioreactors by hand, opened them, and immediately placed 1 ml of sample in a test tube with 10 ml of 0.5 N HCl. We shook the tubes for 1 hour and then allowed the tubes to rest for 1 hour for solids to settle. We removed 1 ml of sample taken from the top of the solution and added the sample to 2.5 ml of 1 g/L ferrozine and 1 M HEPES reagent. We diluted the samples with 0.5 N HCl at twice the dilution factor that we applied to the aqueous ferrous iron samples. We allowed the samples to rest for 1 hour for color development. We obtained the ABS of each sample using a Thermo Scientific Genesys 10S UV-VIS spectrophotometer set at 562 nm. Using linear regression from standards prepared at our lab, we recorded the ferrous iron concentration. If diluted, we applied the dilution factor. We multiplied each value by eleven to account for the HCl to sample dilution to obtain final ferrous iron concentrations.

2.7 Isotopic Analysis

We collected gas samples from all experiments for partial pressures and stable carbon isotopic compositions of CH_4 and CO_2. We sampled our ferric iron mineral and methanogen substrate experiments at the end of the incubation time. We sampled our semi-continuous experiments on the 21st, 35th, and 57th day. Sampling consisted of aseptically withdrawing 5 ml of headspace, replacing the headspace with 5 ml of N_2 gas, and placing the sample into Cali-5-Bond gas bags along with 15 ml of N_2 gas for sample dilution. We mailed these gas bags to Isotech labs for isotopic analyses.

To analyze the samples, Isotech used online continuous-flow GC-IRMS. The data has a precision of +/-0.3 per mil (Isotech Laboratories, 2020). Isotope results are expressed in delta notation relative to Vienna Pee Dee Belemnite (VPDB).

We used these results to evaluate how much methanogenesis occurred in the cultures and the pathway of CH_4 formation. Carbon isotope signatures of CH_4 are a byproduct of kinetic fractionation during methanogenesis, as ^{12}C-substrates are preferentially used over ^{13}C-substrates, leaving the unreacted substrate enriched in ^{13}C (Whiticar et al. 1986; Blair et al., 1987; Blair and Carter, 1992' Whiticar, 1999; Conrad, 2005; Penger et al., 2012). Previous studies have shown that the difference in stable carbon isotope compositions between CO_2 and CH_4 ($\Delta^{13}C = \delta^{13}C\ CO_2 - \delta^{13}C\ CH_4$) can be used as a tracer of the pathway of CH_4 formation (e.g., Smith and Pallasser, 1996; Strąpoć et al., 2007, 2011). Hydrogenotrophic (i.e., CO_2 reduction) and methylotrophic methanogenesis are thought to produce similar isotopic fractionations, which are larger than acetoclastic methanogenesis (Whiticar et al., 1999; Conrad, 2005; Penger et al., 2012). Acetate was the only electron donor supplied in our cultures. Therefore, isotopic compositions consistent with acetatoclastic methanogenesis are consistent with competition

between *G. metallireducens* and *M. barkeri* whereas compositions indicative of hydrogenotrophic methanogenesis imply IET.

2.8 Cell Counts

Brett Nave performed at cell counts at Kansas State University. Brett placed 5 ml of freshly pulled sample into a 25 ml conical vial with a 1% formaldehyde solution and allowed to incubate at 37° for 3 hours. Next, he pipetted the solution onto a black 0.2 μm filter by a vacuum microanalysis vacuum filter holder, rinsed with 10 ml of 18 MΩ DI water, and allowed the filter to dry. He applied a 6% solution of Syto-9 staining reagent to the filter, incubated for 3 minutes in the dark, and rinsed with 10 ml of 18 MΩ DI water, and allowed to dry. Brett placed the filter on glass slide with 100 μl of 4:1 mix of mounting media (Citifluor AF-1:Vectashield), placed a 24 mm X 50 mm superslip over the filter, and sealed the edges with clear nail polish. He then placed the slide on a microscope, took a picture of each quadrant, and used image J to generate a cell count.

To obtain cell counts in units of cell/ml, Brett multiplied the by the filter area in μm^2 divided by the field of view in by the filter area in μm by the cell count number obtained from image J output. He then divided this number by the sample volume of 5 ml to obtain the final value in cell/ml.

Chapter 3 - Results

3.1 Ferric Iron Mineral Experiments

CH_4 generation in ferric iron mineral experiment reactors varied considerably with iron mineralogy and acetate concentration. Reactors with hematite had the highest CH_4 generation relative to acetate supply (Fig. 2A). An average of 242 and 2,051 μmol of CH_4 formed in the 3 and 30 mM acetate cultures with hematite, respectively. CH_4 generation was similar in reactors with goethite, ferrihydrite, and no Fe mineral, with averages ranging from 0 to 74 μmol in 3 mM acetate cultures and 341 to 817 μmol in 30 mM acetate cultures. Reactors with lepidocrocite generated the lowest CH_4, averaging 2 and 94 μmol for 3 and 30 mM acetate cultures, respectively.

Cultures with higher CH_4 generation tended to have lower $\Delta^{13}C$ CO_2-CH_4 values (Fig. 2B). Both conditions of hematite bioreactors produced the lowest $\Delta^{13}C$ CO_2-CH_4 values, averaging 32.3 and 25.7 ‰ at 3 and 30 mM acetate, respectively. $\Delta^{13}C$ CO_2-CH_4 values from goethite, ferrihydrite, and no mineral supplied reactors were relatively similar, with averages ranging from 36.1 to 43.2 ‰ with 3 mM acetate cultures and 34.7 to 40.8 ‰ in 30 mM acetate cultures. Lepidocrocite supplied bioreactors gave the highest $\Delta^{13}C$ CO_2-CH_4 values, averaging 46.3 and 45.1 ‰ for 3 and 30 mM acetate cultures, respectively. There was not enough CH_4 produced in sterile controls and the bioreactors supplied with ferrihydrite alongside 3 mM acetate to obtain $\Delta^{13}C$ CO_2-CH_4 values.

Concentrations of 0.5 N HCl extractable Fe(II) varied with iron mineralogy and acetate concentrations. Sterile controls had significantly less 0.5 N HCl extractable Fe(II) (Fig 3A). Goethite supplied bioreactors generated the most 0.5 N HCl extractable Fe(II), but were similar to ferrihydrite and lepidocrocite supplied bioreactors, with averages ranging from 255.7 to 211.0

µmol at 3 mM acetate and 204.7 to 243.1 µmol at 30 mM acetate. Hematite supplied bioreactors had the lowest 0.5 N HCl extractable Fe(II), with averaging 134.4 and 146.5 µmol at 3 and 30 mM acetate conditions.

Aqueous Fe(II) concentrations varied more strongly with mineralogy than acetate concentration (Fig 3B). Sterile controls had generally less aqueous Fe(II) than cultures with living cells. Lepidocrocite supplied bioreactors generated substantially more aqueous Fe(II) than other reactors, with averages of 33.0 and 3.15 µmol at 3 and 30 mM acetate conditions. Reactors

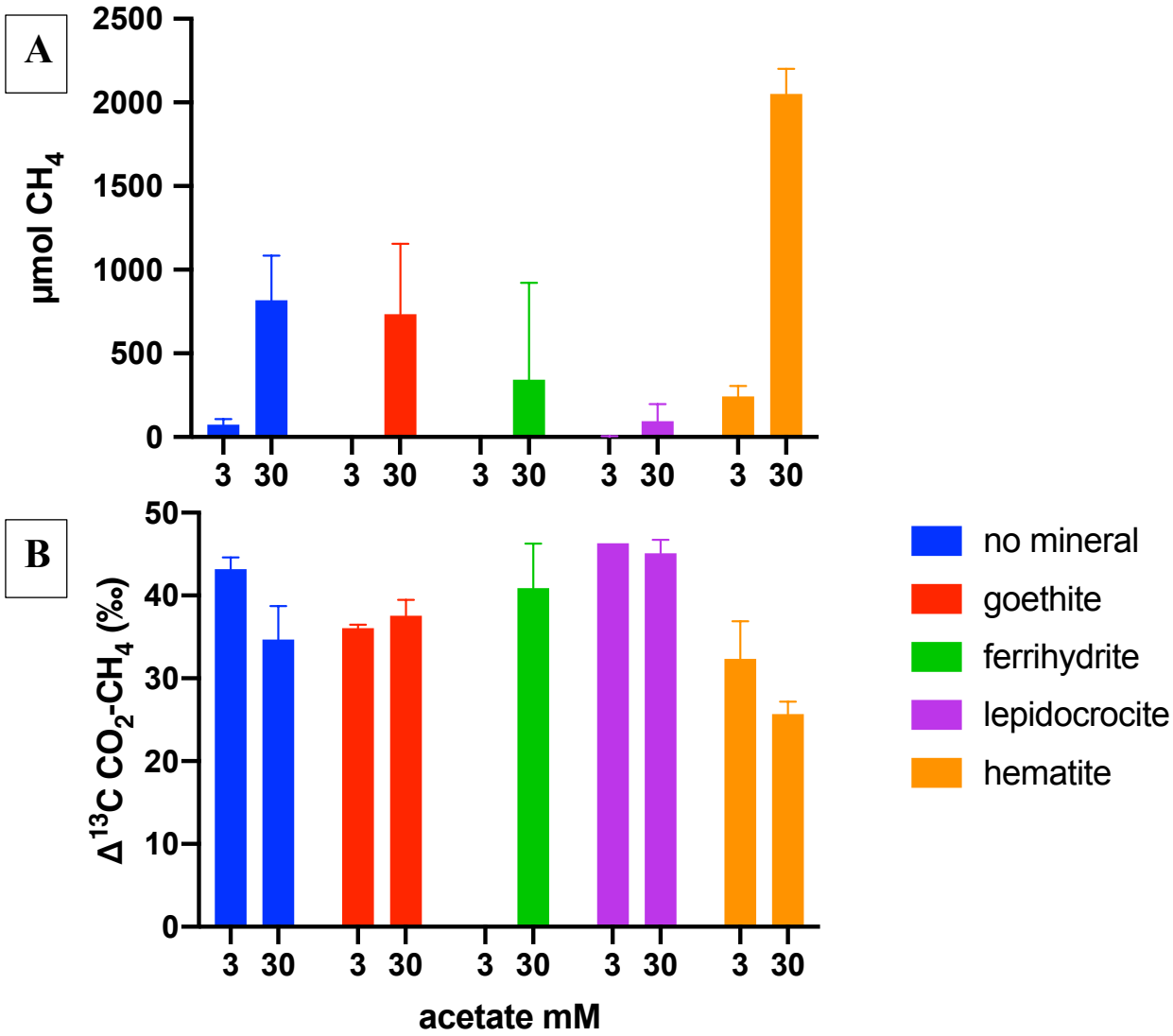

Figure 2 – (A) CH_4 generation and (B) gas isotopic compositions $\Delta^{13}C$ CO_2-CH_4 in the ferric iron mineral experiments relative to VSMOW.

with goethite, ferrihydrite, and hematite produced similar amounts of aqueous Fe(II), giving averages in the range of 3.3 to 7.6 µmol at 3 mM acetate and 5.3 to 9.6 µmol at 30 mM acetate conditions.

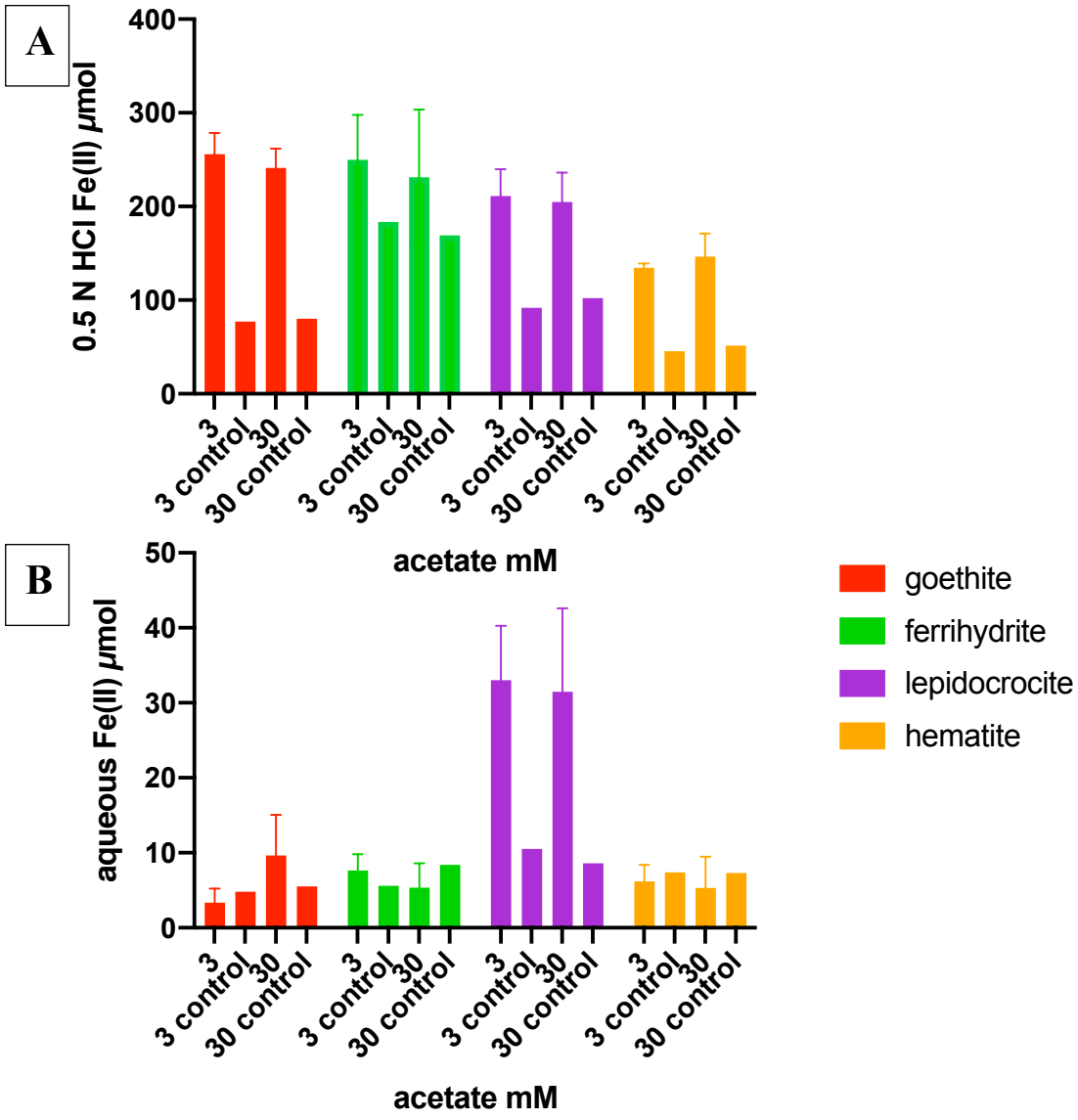

Figure 3 – Variation in (A) 0.5 N HCl extractable Fe(II) and (B) aqueous Fe(II) concentrations in the ferric iron mineral experiments.

The abundance of *G. metallireducen*s cells varied with ferric iron mineralogy and acetate concentrations. Reactors given 30 mM acetate generally generated a higher abundance of *G. metallireducen*s cells over bioreactors given 3 mM acetate (Fig 4A). Reactors supplied with goethite produced the highest abundance of *G. metallireducen*s cells, with averages of 3,283,000 and 3,435,000 cells/ml at 3 and 30 mM acetate. Cell abundances varied widely among cultures without ferric minerals and those with ferrihydrite, lepidocrocite, and hematite, ranging from averages of 95,000 to 3,256,000 cells/ml with 3 mM acetate conditions and 1,177,000 to 3,123,000 cells/ml with 30 mM acetate. At 3 mM acetate conditions, ferrihydrite supplied reactors generated the lowest abundance of cells and at 30 mM acetate conditions hematite produced the lowest cell abundance

Compared to *G. metallireducens*, the abundance of *M. barkeri* varied more strongly with ferric iron mineralogy and acetate concentration. *M. barkeri* cells were more abundant when we supplied bioreactors with 30 mM acetate (Fig 4B). Hematite supplied reactors generated the highest abundance of *M. barkeri* with averages of 12,000 and 562,000 cells/ml at 3 and 30 mM acetate, respectively. Cell counts were similar among cultures without ferric minerals, and those with goethite, and ferrihydrite, with averages ranging from 14,000 to 18,000 cells/ml with 3 mM acetate and 68,000 to 120,000 cells/ml with 30 mM acetate conditions. Lepidocrocite supplied reactors produced the lowest abundance of *M. barkeri* cells, with averages of 0 and 6,000 cells/ml at 3 and 30 mM acetate, respectively.

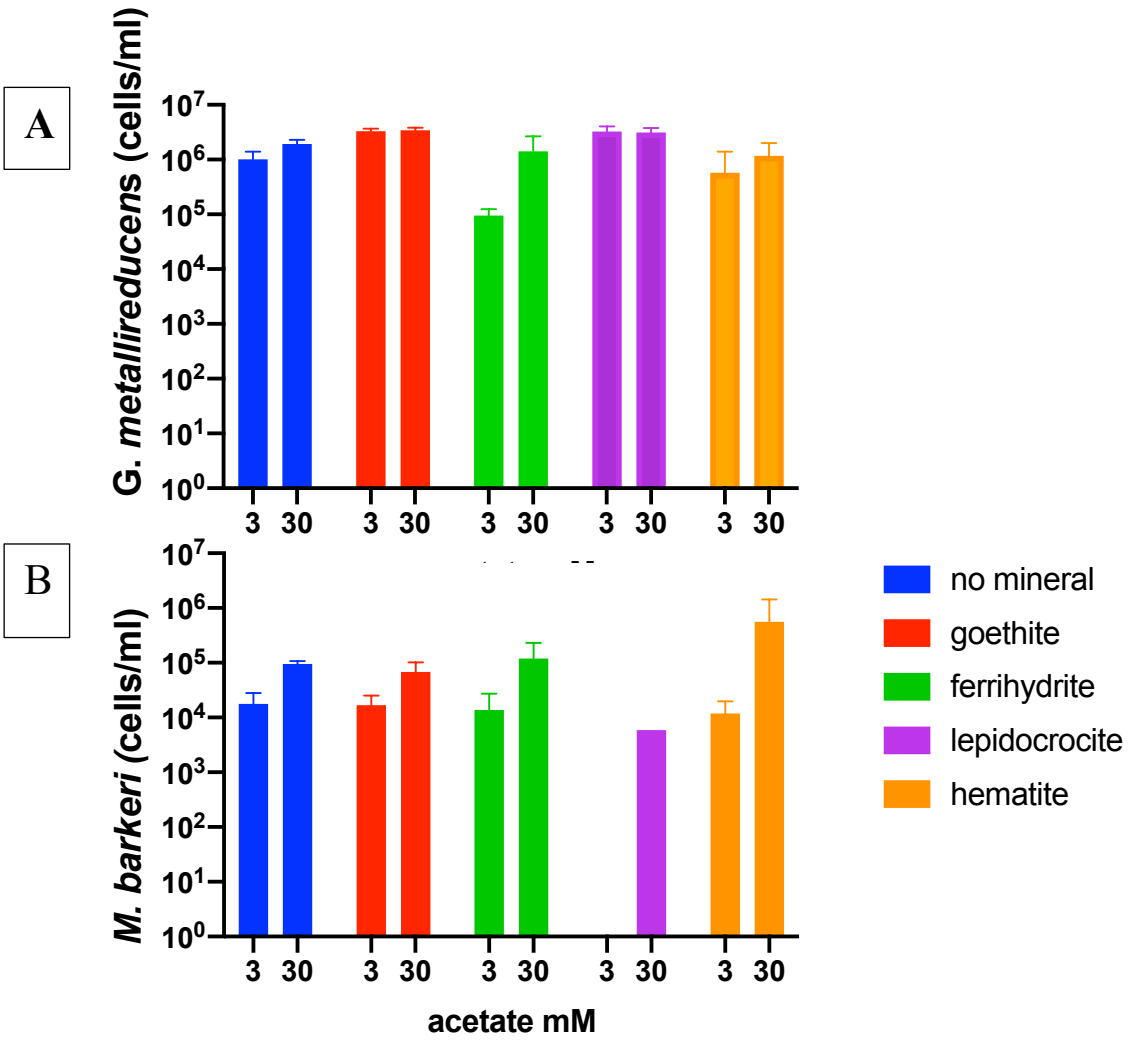

Figure 4 – Variation in (A) G. *metallireducens* and (B) *M. barkeri* cell abundance in ferric iron mineral experiments at the end of the incubation.

3.2 Semi-Continuous Experiments

The final bioreactor pH remained relatively similar with bioreactors supplied 30 mM acetate, while pH of bioreactors supplied with 3 mM acetate dropped an average of approximately 0.1 units after 56 days incubation time (Fig. 5). The pH was consistently higher for bioreactors supplied with 48 mM HCO_3^- over bioreactors given 24 mM HCO_3^-. Bioreactors supplied 48 mM HCO_3^- had starting pH averages of 7.14 and 7.13 at 3 and 30 mM acetate, respectively, and final pH averages of 7.05 and 7.13 with 3 and 30 mM acetate, respectively. Bioreactors given 24 mM HCO_3^- had starting pH averages of 6.97 and 6.96 at 3 and 30 mM acetate, respectively, and the final pH averages of 6.90 and 6.97 at 3 and 30 mM acetate

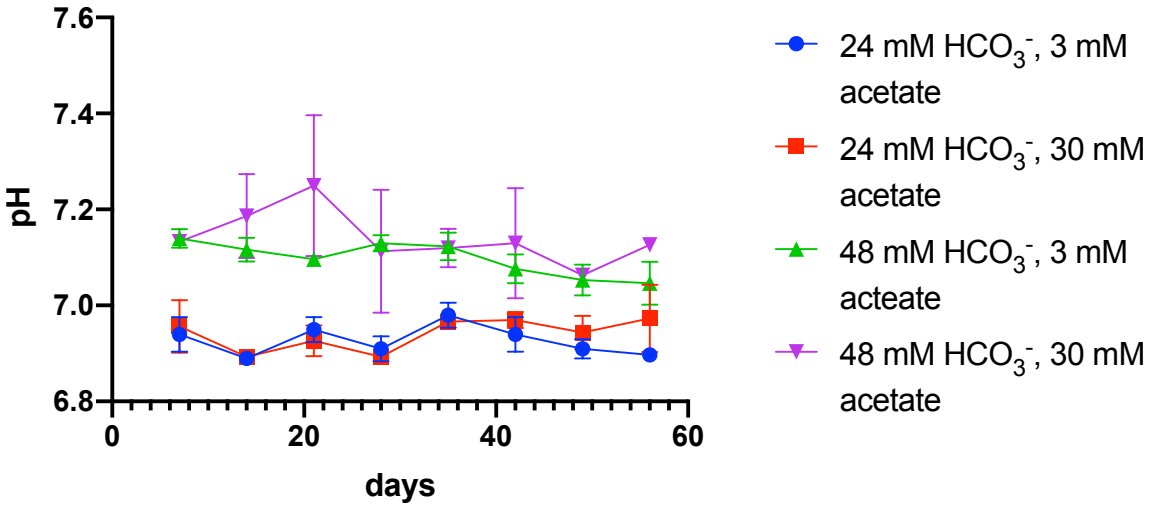

Figure 5 – Variation in pH with time in semi-continuous experiments.

conditions, respectively.

Bioreactor conditions of 24 mM HCO_3^- and 30 mM acetate generated the highest amount of CH_4 (Fig. 6A). Reactors given this condition were the sole ones to continue to generate CH_4 after our second gas sampling, and produced substantially more CH_4 than any other condition, with a final average of 741µmol of CH_4. The remaining three sets of conditions generated final

CH_4 concentrations ranging from 13 to 84 µmol of CH_4, with bioreactors supplied with 48 mM HCO_3^- and 3 mM acetate producing the least amount of CH_4.

The final $\Delta^{13}C$ CO_2-CH_4 values generally decreased with higher CH_4 production (Fig. 6B). Bioreactors supplied with 24 mM HCO_3^- and 30 mM acetate gave the highest initial average $\Delta^{13}C$ value of 38.1 ‰, and the lowest final $\Delta^{13}C$ CO_2-CH_4 value of 29.1‰. This was the sole condition that had a substantial decrease in $\Delta^{13}C$ values through time. The $\Delta^{13}C$ values of the

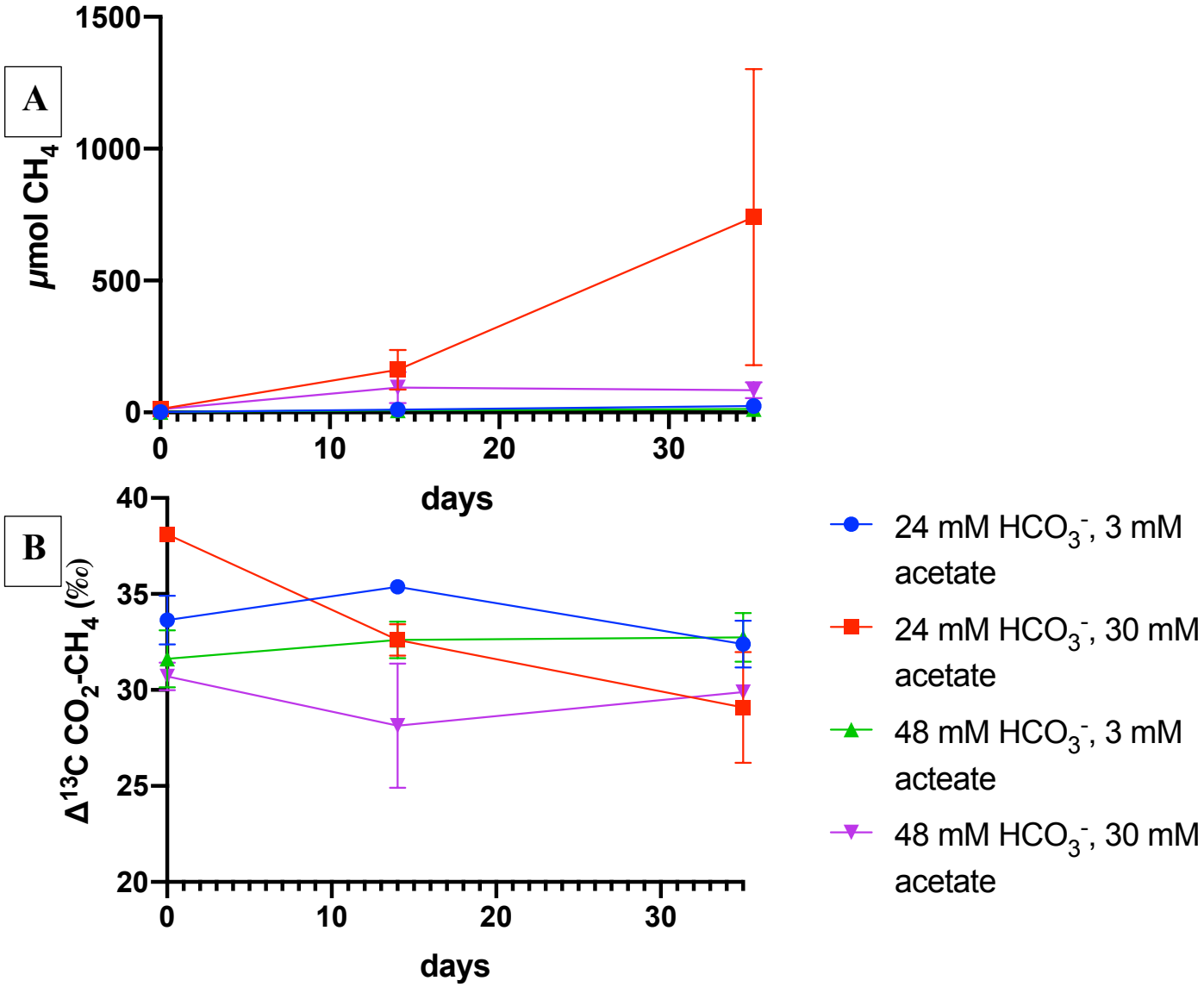

Figure 6 – Variation over time of (A) CH_4 produced and (B) $\Delta^{13}C$ CO_2-CH_4 in semi-continuous experiments

remaining three conditions behaved relatively similar with initial $\Delta^{13}C$ CO_2-CH_4 values ranging from 30.7 to 33.6 ‰ and final $\Delta^{13}C$ values ranging from 29.9 to 32.7 ‰.

The average abundance of *G. metallireducen*s cells was initially relatively similar for all conditions, decreased at 28 days, then cultures supplied with 24 mM HCO_3^- increased *G. metallireducen*s cell abundance while cultures supplied with 48 mM HCO_3^- continued to decrease *G. metallireducen*s cell abundance (Fig 7A). Cell counts of *G. metallireducen*s ranged

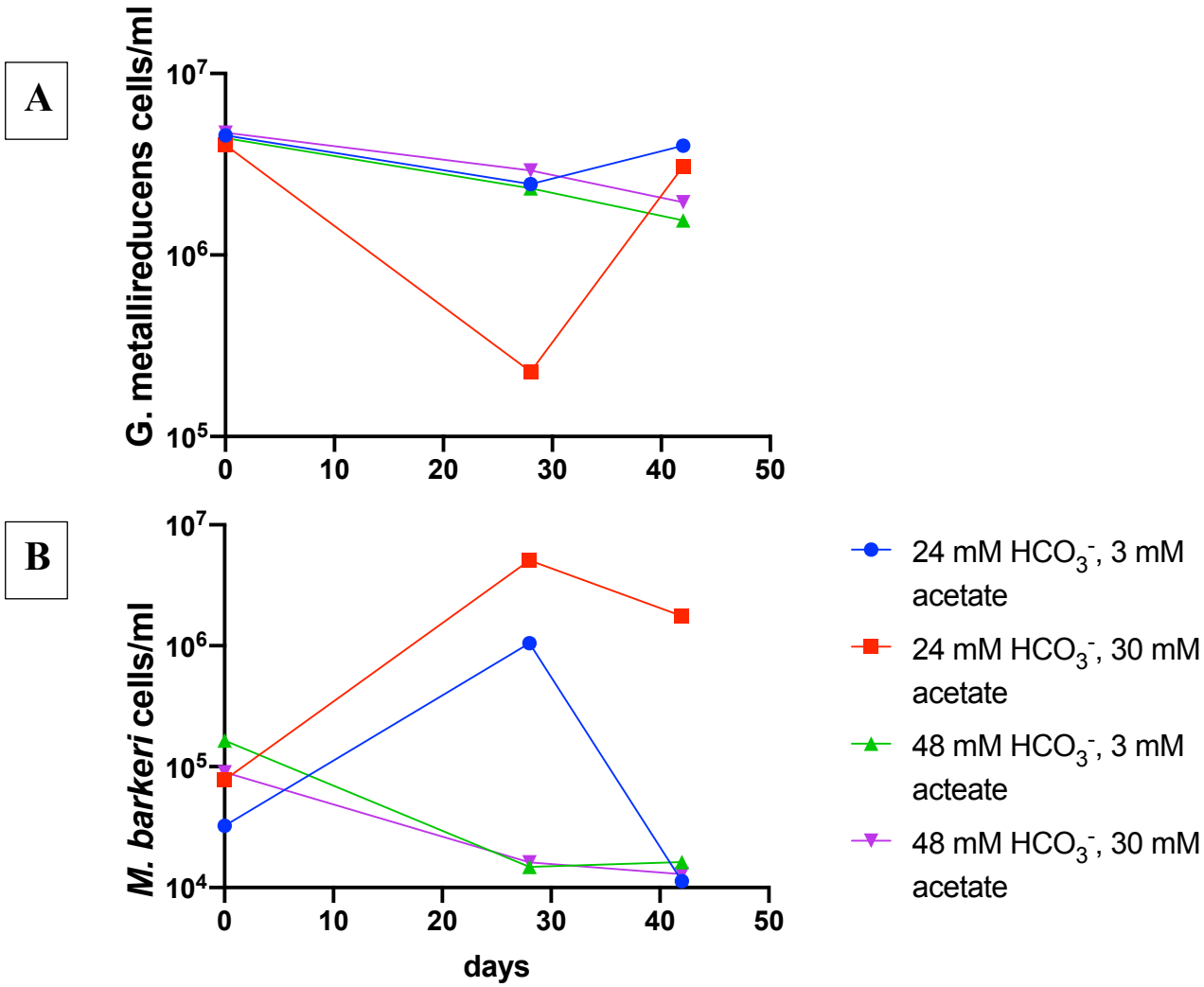

Figure 7 –Variation over time of (A) G. *metallireducen*s and (B) *M. barkeri* cell abundance in semi-continuous experiments

from 4,029,000 to 4,724,000 cells/ml initially, from 28,000 to 2,917,000 cells/ml at our second counting event, and from 1,550,000 to 4,011,000 cells/ml at the end of incubation.

Oppositely of *G. metallireducen*s cell abundance, the average cell counts of *M. barkeri* cultures supplied with 24 mM HCO_3^- increased in abundance after 28 days, then decreased at 48 days (Fig 7B). At the end of incubation, cultures supplied with 24 mM HCO_3^- and 30 mM acetate had substantially more *M. barkeri* cells than other conditions, with 1,764,000 cells/ml, while other conditions ranged from 11,000 to 16,000 cells/ml. *M. barkeri* cell abundance in cultures supplied with 48 mM HCO_3^- steadily declined with time, giving initial ranges of 90,000 to 165,000 cells/ml and final cell counts of 12,000 to 16,000 cells/ml.

3.3 Methanogen Substrate Experiments

CH_4 generation varied with the pathway utilized. Reactors supplied with acetate yielded the highest CH_4 concentrations followed by methanol and H_2 (Fig. 8A). Stoichiometry of the reactions varied with the substrate (Table 2). Based on reaction stoichiometry, hydrogenotrophic methanogenesis was limited by hydrogen supply. The CH_4 produced (111 μmol) would require virtually all of the hydrogen supplied. In contrast, only consumption of about 8 and 5% of the electron donor was necessary to produce the CH_4 in the acetate and methanol cultures, respectively.

Similar to the results obtained from ferric iron mineral experiments and semi-continuous experiments, $\Delta^{13}C$ CO_2-CH_4 values generally decreased with increasing CH_4 production (Fig 8B). The highest $\Delta^{13}C$ CO_2-CH_4 values came from bioreactors supplied with H_2 with a mean of 32.7 ‰, followed by methanol supplied bioreactors with a mean of 31.6 ‰, and acetate with the lowest $\Delta^{13}C$ values averaging 21.3 ‰.

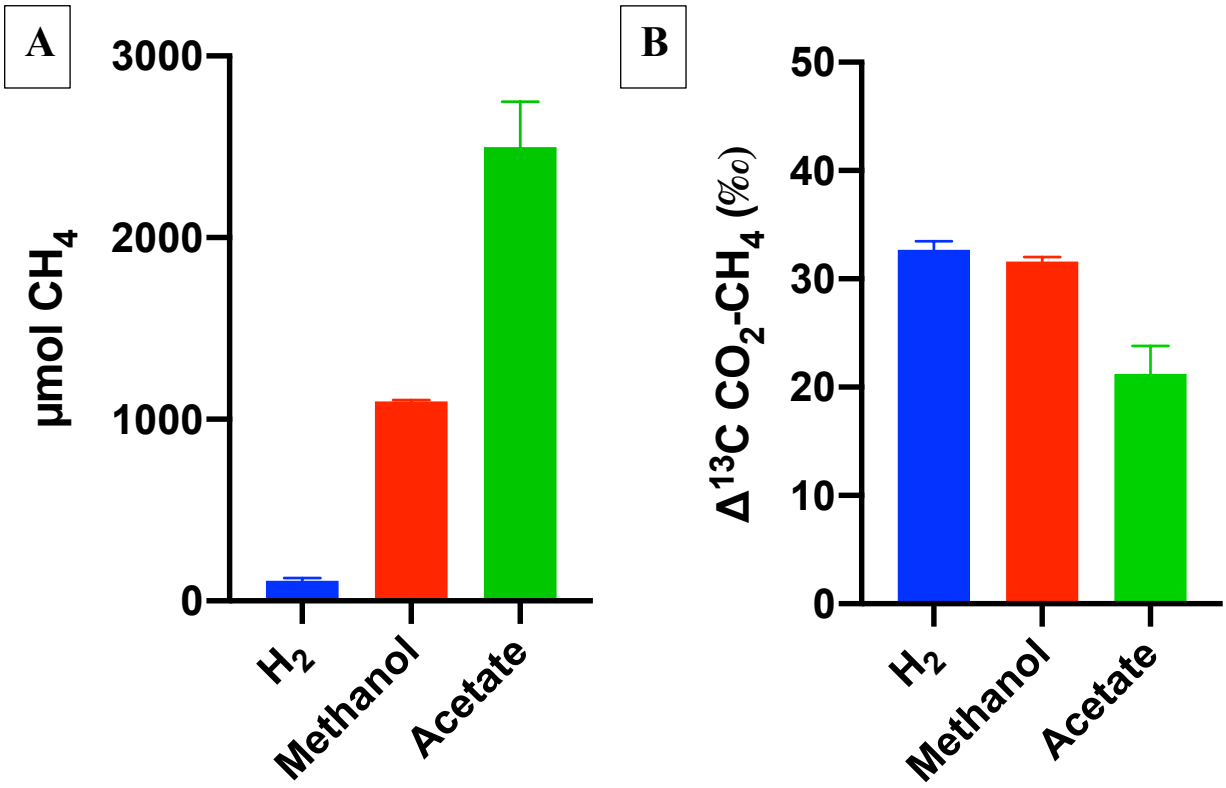

Figure 8 – Variation in (A) CH_4 produced and (B) $\Delta^{13}C$ CO_2-CH_4 in methanogen substrate experiments.

Table 2 – Reactions for methanogenic pathways

Reaction	Equation
Acetoclastic methanogenesis	$CH_3COO^- + H^+ \rightarrow CO_2 + CH_4$
Hydrogentrophic methanogenesis	$H_2 + 0.25\ CO_2 \rightarrow 0.25\ CH_4 + 0.5\ H_2O$
Methylotrophic methanogenesis	$CH_3OH \rightarrow 0.75\ CH_4 + 0.25\ CO_2 + 0.5\ H_2O$

Chapter 4 - Discussion

4.1 Extents of Reactions

We evaluate the extent of iron reduction based on the extractable Fe, which includes dissolved Fe(II) as well as Fe(II) that is sorbed and any that may have precipitated with carbonate or phosphate (Heron et al. 1994). Bioreactors provided with goethite generated the most 0.5 N HCl extractable Fe(II) but with similar concentrations to ferrihydrite and lepidocrocite. Reactors with hematite supplied the least amount of 0.5 N HCL extractable Fe(II). Im et al. (2013) demonstrated that the presence of Fe^{3+} causes over-estimation in Fe^{2+} concentrations and this discrepancy increases linearly with incubation time. Thus, the total reduced iron values calculated for this experiment are likely overestimated.

Variation in the extent of iron reduction with culture mineralogy likely reflects differences in mineral stability. Poorly crystalline phases such as ferrihydrite ($Fe(OH)_3$) tend to have higher surface areas and solubilities than more stable phases, such as goethite (FeO(OH)) and hematite (Fe_2O_3). Iron reduction rates have been found to increase with (oxyhdr)oxide surface area and solubility (Larsen and Postma, 2001; Roden, 2003, 2006; Bonneville et al., 2004, 2009; Cutting et al., 2009). The amount of 0.5 N HCl Fe(II) generated corresponded with the energy available to G. *metallireducen*s from the ferric iron mineral supplied (Fig 1). Hematite was the most stable ferric iron mineral used in our experiments and these cultures generated the least amount of 0.5 N HCl extractable Fe(II), with 134 μmol and 147 μmol at 3 and 30 mM acetate. The other ferric iron minerals in our experiments generated at least 205 μmol of 0.5 N HCl extractable Fe(II) under all conditions.

In contrast to iron reduction, the extent of methanogenesis was higher in cultures with more stable ferric minerals. Relative to CH_4 production in the absence of a ferric iron mineral, at 74

and 817 μmol at 3 and 30 mM acetate, respectively, the presence of hematite increased CH_4 production, generating 242 and 2,051 μmol of CH_4 with 3 and 30 mM acetate, while the presence of other ferric iron minerals suppressed CH_4 generation. This may reflect variation in the level of competition between *G. metallireducens* and *M. barkeri* but also the extent of cooperation between each species.

Our results suggest that G. *metallireducenss* and M. *barkeri* responded differently to variation in acetate supply. Although CH_4 generation increased considerably with acetate supply, the extent of iron reduction changed little. These results likely reflect differences in the enzyme kinetic properties between the two species. Methanogenic microorganisms typically have higher half-saturation constants than iron-reducing species (Bethke et al. 2008). As a result, methanogens require greater concentrations of substrate than iron reducers to run their metabolic reaction rapidly. Therefore, methanogenesis would have benefited more than iron reduction from higher acetate concentration, consistent with the results we observed.

Variation in CH_4 generation in the semi-continuous cultures may reflect differences in the role of bicarbonate in methanogenic pathways. As noted in the introduction, acetoclastic methanogenesis generates bicarbonate:

$$CH_3COO^- + H_2O \leftrightarrow HCO_3^- + CH_4(aq)$$

In contrast, hydrogenotophic methanogenesis consumes inorganic carbon, as shown in the following example reaction written in terms of bicarbonate:

$$H_2(aq) + 0.25\ H^+ + 0.25\ HCO_3^- \leftrightarrow 0.25\ CH_4(aq) + 0.75\ H_2O$$

Thus, added bicarbonate makes acetoclastic methanogenesis less favorable but increases the favorability of hydrogenotrophic methanogenesis. Given that IET, like hydrogenotrophic methanogenesis, consumes inorganic carbon, these relationships may explain why we see the

greatest CH_4 generation in cultures with the lowest bicarbonate (24 mM bicarbonate + 30 mM acetate). Those cultures also had the lowest $\Delta^{13}C$ CO_2-CH_4 values, consistent with the largest contribution from acetoclastic methanogenesis among semi-continuous cultures.

4.2 Pathway

In our methanogen substrate experiments, we saw distinct $\Delta^{13}C$ CO_2-CH_4 values for methanogenesis utilizing hydrogen or methanol as an elector donor compared to acetoclastic methanogenesis. The $\Delta^{13}C$ CO_2-CH_4 values from most of our coculture experiments points to CH_4 produced from hydrogentrophic methanogenesis. However, we did not supply H_2 and G. *barkeri* is not capable of producing H_2 from acetate. Hence, we propose these $\Delta^{13}C$ CO_2-CH_4 values originated from IET occurring.

Cell count data in coculture experiments without a ferric iron mineral present support the occurrence of IET. If competition was solely occurring in our bioreactors, G. *metallireducen*s cells would be not have a pathway to grow in the absence of a ferric iron mineral. Ferric iron mineral experiments omitting a ferric iron mineral produced G. *metallireducen*s average cell counts of 1,020,000 and 1,936,000 cells/ml in bioreactors given 3 and 30 mM acetate, respectively. This is a substantially higher abundance of cells relative to the initial abundance 22,5000 cells/ml and a higher cell count average than in bioreactors supplied with ferrihydrite, with 95,000 cells/ml and 1.42 million cells/ml at 3 and 30 mM acetate, respectively, and hematite, with 575,000 and 1,176,000 cells/ml at 3 and 30 mM acetate. Furthermore, our semi-continuous experiments did not contain a ferric iron mineral and G. *metallireducen*s cell counts were above 4,000,000 cells/ml for all conditions for our cell count after 14 days of incubation.

In our ferric iron mineral experiments, hematite supplied cultures with 30 mM acetate gave $\Delta^{13}C$ CO_2-CH_4 values consistent with aectoclastic methanogenesis and generated substantially

more CH_4 and *M. barkeri* cells/ml than the cultures supplied with any other ferric mineral and cultures with no ferric mineral. Gas samples from the reactors with hematite and 30 mM acetate gave $\Delta^{13}C$ CO_2-CH_4 values averaging 25.7 ‰. This was the lowest $\Delta^{13}C$ CO_2-CH value from our ferric mineral experiments and closest value to our acetoclastic $\Delta^{13}C$ CO_2-CH value of 21.3 ‰ in our methanogen substrate experiments. Reactors with hematite and 30 mM acetate averaged 562,000 *M. barkeri* cells/ml compared to the next highest abundances of 120,000 cells/ml in ferrihydrite reactors and 95,000 cells/ml in reactors with no mineral present. CH_4 production was substantially higher with hematite and 30 mM acetate compared to other conditions. These reactors produced an average of 2,051 µmol of CH_4, with the next highest condition producing 817 µmol of CH_4. We propose acetoclastic methanogenesis was the dominant pathway utilized for these conditions resulting in CH_4 generation and M. barkeri growth to be the greatest when they didn't have to share some of the energy with G. metallireducences.

4.3 Implications

The environmental significance of IET is not well known. Results suggest IET may be very common, depending on the types of ferric iron minerals available. Environmental pH may also play an important role in determining which pathway iron reducers and methanogens utilize (Marquart et al. 2018). Our findings suggest that IET may be very common in the natural world and demonstrates that ferric iron mineralogy, electron donor concentrations, and alkalinity play a role in determining which metabolic pathway is utilized. Our findings may aid further development in stable isotope methods to better understand the occurrence of IET in methanogenic systems.

If our interpretation of stable isotope results is correct, it may shed light on a puzzling question: where does the acetate go in natural gas reservoirs? In many coal and shale-gas reservoirs, stable isotopes of the natural gas are consistent with CH_4 formed primarily by H_2 oxidation coupled with CO_2 reduction. However, organic matter degradation would be expected to produce acetate as well as H_2 as a terminal product (Conrad, 1999). Where has it gone? Our results suggest that it may have been funneled to methanogenesis via IET. As a result, the stable isotope compositions of the gas are consistent with CO_2 reduction (Vinson et al., 2017; Golding et al., 2013). If this is true, it would mean that IET is a major process linked to our energy supply and it implies a strong environmental relevance for IET.

Chapter 5 - Conclusion

Iron reduction and methanogenesis play a vital role in shaping the natural world. Their interactions can be complex and controls on these interactions are poorly understood. Our experiments show that ferric iron mineralogy, acetate, and HCO_3^- concentrations have a role in variations on these interactions. Carbon stable isotope compositions ($\delta^{13}C$) of CO_2 and CH_4 from both culturing experiments suggest that differences in methane generation between cultures may in part reflect variation in the pathway of methanogenesis. Our results provide a possible explanation on acetate consumption in the natural world and why stable isotopes of CH_4 of coal and shale-gas reservoirs rarely point to acetoclastic methanogenesis.

These results provide compelling evidence that there was variation in the pathway of methanogenesis and that IET may have played a dominant role in CH_4 generation. However, our understanding of the stable isotope implications of IET are limited. There is uncertainty about how the isotope separation would change with substrate use and in response to inorganic carbon production by *G. metallireducens* and *M. barkeri.* More research is needed to identify impacts of IET on the carbon isotope systematics.

References

Achtnich, C., Bak, F., & Conrad, R. (1995). Competition for electron donors among nitrate reducers, ferric iron reducers, sulfate reducers, and methanogens in anoxic paddy soil. Biology and Fertility of Soils. 19, 65-72. https://doi.org/10.1007/BF00336349

Aklujkar, M., Krushkal, J., DiBartolo, G., Lapidus, A., Land, M. L., & Lovley, D. R. (2009). The genome sequence of Geobacter metallireducens: Features of metabolism, physiology and regulation common and dissimilar to Geobacter sulfurreducens. *BMC Microbiology*, *9*(1), 109. https://doi.org/10.1186/1471-2180-9-109

Appels, L., Baeyens, J., Degreve, J., & Dewil, R., (2008) Principles and potential of the anaerobic digestion of waste-activated sludge. Progress in Energy and Combustion Science, 34(6), 755–781.

Bethke, C. M., & Johnson, T. M. (2008). Groundwater Age and Groundwater Age Dating. *Annual Review of Earth and Planetary Sciences*, *36*(1), 121–152. https://doi.org/10.1146/annurev.earth.36.031207.124210

Bethke, C. M., Sanford, R. A., Kirk, M. F., Jin, Q., & Flynn, T. M. (2011). The thermodynamic ladder in geomicrobiology. American Journal of Science, 311(3), 183-210. https://doi.org/10.2475/03.2011.01

Blair, N.E., Carter, W.D., (1992). The carbon isotope biogeochemistry of acetate from a methanogenic marine sediment. Geochim. Cosmochim. Acta 56, 1247–1258.

Blair, N., Martens, C., Des Marais, D., (1987). Natural abundances of carbon isotopes in acetate from a coastal marine sediment. Science 236:66–68. http://doi.org/10.1126/science.11539717

Bonneville, S., Van Cappellen, P., & Behrends, T. (2004). Microbial reduction of iron(III) oxyhydroxides: Effects of mineral solubility and availability. *Chemical Geology*, *212* (3-4), 255–268. https://doi.org/10.1016/j.chemgeo.2004.08.015

Bonneville, S., Behrends, T., & Van Cappellen, P. (2009). Solubility and dissimilatory reduction kinetics of iron(III) oxyhydroxides: A linear free energy relationship. *Geochimica et Cosmochimica Acta*, *73*(18), 5273–5282. https://doi.org/10.1016/j.gca.2009.06.006

Conklin, A., Stensel, H. D., & Ferguson, J. (2006). Growth Kinetics and Competition Between Methanosarcina and Methanosaeta in Mesophilic Anaerobic Digestion. Water Environment Research, 78(5), 486–496. https://doi.org/10.2175/106143006X95393

Conrad, R. (1999). Contribution of hydrogen to methane production and control of hydrogen concentrations in methanogenic soils and sediments. FEMS Microbiology Ecology, 10.

Conrad, R., (2005). Quantification of methanogenic pathways using stable carbon isotopic signatures: a review and a proposal. Org. Geochem. 36:739–752. https://doi.org/10.1016/j.orggeochem.2004.09.006

Cornell, R. M., Schwertmann, U. (2003). Iron oxides in the laboratory: Preparation and Characterization. New York, NY: Wiley-VCH. https://doi.org/10.1002/3527602097

Cutting, R. S., Coker, V. S., Fellowes, J. W., Lloyd, J. R., & Vaughan, D. J. (2009). Mineralogical and morphological constraints on the reduction of Fe(III) minerals by Geobacter sulfurreducens. *Geochimica et Cosmochimica Acta*, *73*(14), 4004–4022. https://doi.org/10.1016/j.gca.2009.04.009

Emerson, D., Roden, E., & Twining, B. S. (2012) The microbial ferrous wheel: Iron Cycling in terrestrial, freshwater and marine environments. Frontiers in Microbiology, 3, 383.

Forster, P., Ramaswamy, V., Artaxo, P., Berntsen, T., Betts, R., Fahey, D. W., Haywood, J., Lean, J., Lowe, D. C., Raga, G., Schulz, M., Dorland, R. V., Bodeker, G., Etheridge, D., Foukal, P., Fraser, P., Geller, M., Joos, F., Keeling, C. D., … Dorland, R. V. (n.d.). Changes in Atmospheric Constituents and in Radiative Forcing. 106.

Flynn, T. M., Sanford, R. A., Ryu, H., Bethke, C. M., Levine A. D., Ashbolt, N. J., & Santo Domingo J.W. (2013). Functional microbial diversity explains groundwater chemistry in a pristine aquifer. BMC Microbiology. 13, 146. https://doi.org.10.1186/1471-2180-13-146

Golding, S.D., Boreham, C.J., Esterle, J.S., (2013). Stable isotope geochemistry of coal bed and shale gas and related production waters: a review. Int. J. Coal Geol. 120:24–40. https://doi.org/10.1016/j.coal.2013.09.001

Gujer, W., & Zehnder, A. J. B. (1983). Conversion Processes in Anaerobic Digestion. Water Science and Technology, 15(8–9), 127–167. https://doi.org/10.2166/wst.1983.0164

Hander, R. M., Beard, B. L., Johnson, C. M., & Schere, M. M. (2009). Atom exchange between aqueous Fe(II) and Goethite: An Fe isotope tracer study. Environmental Science and Technology, 43(4), 1102-1107. https://doi.org.10.1021/es802402m

Herndon, E. M., Yang, Z. M., Bargar, J., Janot, N., Regier, T., Graham, D., Wullschleger, S. D., Gu, B., & Liang, L. Y. (2015). Geochemical drivers of organic matter decomposition in arctic tundra soils. Biogeochemistry, 126, 397-414. https://doi.org/10.1007/s10533-015-01655

Heron, Gorm., Crouzet, Catherine., Bourg, A. C. M., & Christensen, T. H. (1994). Speciation of Fe(II) and Fe(III) in Contaminated Aquifer Sediments Using Chemical Extraction Techniques. *Environmental Science & Technology*, *28*(9), 1698–1705. https://doi.org/10.1021/es00058a023

Im, J., Lee, J., & Löffler, F. E. (2013). Interference of ferric ions with ferrous iron quantification using the ferrozine assay. Journal of Microbiological Methods, 95(3), 366–367. https://doi.org/10.1016/j.mimet.2013.10.005

Isotech Laboratories, Inc. (2020). Analytical Services > View by Isotope > Carbon https://www.isotechlabs.com/analytical/isotope/carbon.html

Jakobsen, R., & Postma, D. (1999). Redox zoning, rates of sulfate reduction and interactions with Fe-reduction and methanogenesis in a shallow sandy aquifer, Romo, Denmark. Geochimica et Cosmochimica Acta, 63, 137-151. https://doi.org/10.1016/S00016-7037(98)00272-5

Jin, Q., & Kirk, M. F. (2018). pH as a primary control in environmental microbiology: 1. Thermodynamic perspective. Frontiers in Environmental Science, 6, 1-15. https://doi.org/10.3389/fenvs.2018.00021.

Kirk, M. F., Santillan, E. F. U., Sanford, R. A., & Altman S. J. (2013) CO_2 induced shift in microbial activity affects carbon trapping and water quality in anoxic bioreactors. Geochimica et Cosmochimica Acta, 122, 198–208. https://doi.org/10.1016/j.gca.2013.08.018

Kirschke, S., Bousquet, P., Ciais, P., Saunois, M., Canadell, J. G., Dlugokencky, E. J., Bergamaschi, P., Bergmann, D., Blake, D. R., Bruhwiler, L., Cameron-Smith, P., Castaldi, S., Chevallier, F., Feng, L., Fraser, A., Heimann, M., Hodson, E. L., Houweling, S., Josse, B., … Zeng, G. (2013). Three decades of global methane sources and sinks. *Nature Geoscience*, *6*(10), 813–823. https://doi.org/10.1038/ngeo1955

Küsel, K., Blöthe, M., Shculz, D., Reiche, M., & Drake, H. L. (2008). Microbial reduction of iron and porewater biogeochemistry in acidic peatlands. Biogeosciences, 5. 1537-1549. https://doi.org/10.5194/bg-5-1537-2008

Lareses-Casanova, P., Scherer M. M. (2007). Sorption on hematite: New insights based on spectroscopic measurements. Environmental Science and Technology. 41(2), 471-477. https://doi.org/10.1021/es0617035

Larsen O, Postma D (2001) Kinetics of reductive bulk dissolution of lepidocrocite, ferrihydrite, and goethite. *Geochimica Et Cosmochimica Acta* **65**, 1367–1379. https://doi.org/10.1016/S0016-7037(00)00623-2

Liu, F.; Rotaru, A.-E.; Shrestha, P. M.; Malvankar, N. S.; Nevin, K. P.; Lovley, D. R. (2012). Promoting direct interspecies electron transfer with activated carbon. *Energy Env. Sci.*, *5* (10), 8982-8989 https://doi.org/10.1073/pnas.1117592109

Liu, Y., Boone, D. R., Sleat, R., & Mah, R. A. (1985). Methanosarcina mazei LYC, a New Methanogenic Isolate Which Produces a Disaggregating Enzyme. Applied and Environmental Microbiology, 49(3), 608–613. https://doi.org/10.1128/AEM.49.3.608-613.1985

Lovley, D.R. (1995). Deep Subsurface Microbial Processes. Reviews of Geophysics, 33(3), 365-381.

Lovley, D. R. (1991). Dissimilatory Fe(III) and Mn(IV) Reduction. *MICROBIOL. REV.*, *55*, 29.

Lovley, D. R. (2017). Happy together: Microbial communities that hook up to swap electrons. ISME Journal, 11, 327-336. https://doi.org/10.1038/ismej.2016.136

Lovley, D. R., & Goodwin, S. (1988). Hydrogen concentrations as an indicator of the predominant terminal electron-accepting reactions in aquatic sediments. Geochimica et Cosmochimica Acta, 52, 2993-3003. https://doe.org/10.1016/0016-7037(88)90163-9

Marquart K. A., Haller B. R., Paper J. M., et al. (2018). Influence of pH on the balance between methanogenesis and iron reduction. Geobmicrobiology. 2018;00:1-14. https://doi.org/10.1111/gbi.12320

Melton, E. D., Swanner, E. D., Behrens, S., Schmidt, C., & Kapler, A. (2014). The interplay of microbially mediated and abiotic reactions in the biogeochemical Fe cycle. Nature Reviews Microbiology, 12, 797-808. https://doi.org/10.1038/nrmicro3347

Metje, M., & Frenzel, P. (2007). Methanogenesis and methanogenic pathways in a peat from subartic permafrost. Environmental Microbiology, 9, 954-964. https://doi.org/10.1111/j.1462-2920.2006.01217.x

Milkov A. V. (2011). Worldwide distribution and significance of secondary microbial methane formed during petroleum biodegradation in conventional reservoirs. Organic Geochemistry, 42:2, 184-207, https://doi.org/10.1016/j.orggeochem.2010.12.003

Paul S., Küsel, K., & Alewell, C. (2006). Reduction processes in forest wetlands: Tracking down heterogeneity of source/sink functions with a combination of methods. Soil Biology & Biochemistry, 38, 1028-1039. https://doi.org/10.1016/j.soilbio.2005.09.001

Penger, J., Conrad, R., Blaser, M., (2012). Stable carbon isotope fractionation by methylotrophic methanogenic Archaea. Appl. Environ. Microbiol. 78:7596–7602. https://doi.org/10.1128/AEM.01773-12

Reiche, M., Torburg, G., & Küsel, K. (2008). Competition of Fe(III) reduction and methanogenesis in an acidic fen. FEMS Microbiology Ecology, 65, 88-101. https://doi.org/10.1111/j.1574-6941.2008.00523.x

Roden, E. E. (2003). Fe(III) Oxide Reactivity Toward Biological versus Chemical Reduction. *Environmental Science & Technology*, *37*(7), 1319–1324. https://doi.org/10.1021/es026038o

Roden, E. E. (2006). Geochemical and microbiological controls on dissimilatory iron reduction. *Comptes Rendus Geoscience*, *338*(6–7), 456–467. https://doi.org/10.1016/j.crte.2006.04.009

Rosso, K. M., Yanina, S. V., Gorski, C. A., Larese-Casanova, P., & Scherer, M. M. (2010). Connecting observations of hematite (α-Fe2O3) growith catalyzed by Fe(II). Environmental Science and Technology, 44(1), 61-67. https://doi.org/10.1021/es901882a

Rotaru, A. E., Shrestha P.M., Liu F., Markovaite B., Chen, S., Nevin, K. P., & Lovley, D. R. (2014a). "Direct Interspecies Electron Transfer between Geobacter Metallireducens and Methanosarcina Barkeri." Edited by G. Voordouw. Applied and Environmental Microbiology 80 (15): 4599–4605. https://doi.org/10.1128/AEM.00895-14.

Rotaru, A. E., Shrestha, P. M., Liu, F. H., Shrestha, M., Shrestha, D., Embree, M., Zengler K., Wardman, C., Nevin K. P. & Loveley, D. R. (2014b). A new model for electron flow during anaerobic digestion: Direct interspecies electron transfer to Methonsaeta from the reduction of carbon dioxide to methane. Energy & Environmental Science. 7. 408-415. https://doi.org/10.1039/C3EE42189A

Shin, S. G., Zhou, B. W., Lee, S., Kim, W., & Hwang, S. (2011). Variations in methanogenic population structure under overloading of pre-acidified high-strength organic wastewaters. Process Biochemistry, 46(4), 1035–1038. https://doi.org/10.1016/j.procbio.2011.01.009

Smith, J.W., Pallasser, R.J., (1996). Microbial origin of Australian coalbed methane. AAPG Bull. 80, 891–897.

Stookey, L. L. (1970). Ferrozine—A new spectrophotometric reagent for iron. Analytical Chemistry, 42(7), 779–781. https://doi.org/10.1021/ac60289a016

Strąpoć, D., Mastalerz, M., Dawson, K., Macalady, J., Callaghan, A. V., Wawrik, B., Turich, C., & Ashby, M. (2011). Biogeochemistry of Microbial Coal-Bed Methane. *Annual Review of Earth and Planetary Sciences*, *39*(1), 617–656. https://doi.org/10.1146/annurev-earth-040610-133343

Strąpoć, D., Mastalerz, M., Eble, C., & Schimmelmann, A. (2007). Characterization of the origin of coalbed gases in southeastern Illinois Basin by compound-specific carbon and hydrogen stable isotope ratios. *Organic Geochemistry*, *38*(2), 267–287. https://doi.org/10.1016/j.orggeochem.2006.09.005

Thauer R. K., Kaster A. K., Seedorf H., Buckel W., & Hedderich R. (2008) Methanogenic archae: Ecologically relevant differences in energy conservation. Nature Reviews Microbiology, 6, 579-591. https://doi.org/10.1038/nrmicor1931

Vinson, D. S., Blair, N. E., Martini, A. M., Larter, S., Orem, W. H., & McIntosh, J. C. (2017). Microbial methane from in situ biodegradation of coal and shale: A review and reevaluation of hydrogen and carbon isotope signatures. Chemical Geology, 453, 128–145. https://doi.org/10.1016/j.chemgeo.2017.01.027

Weber, K. A., Achenbach, L. A., & Coates J. D. (2006). Microorganisms pumping iron: anaerobic microbial iron oxidation and reduction. Nature Reviews Microbiology, 4:10, 752-764. https://doi.org/10.1038/nrmicro1490

Whiticar, M.J., (1999). Carbon and hydrogen isotope systematics of bacterial formation and oxidation of methane. Chem. Geol. 161:291–314. https://doi.org/10.1016/S00092541(99)00092-3

Whiticar, M.J., Faber, E., (1986). Methane oxidation in sediment and water column environments—isotope evidence. Org. Geochem. 10:759–768. https://doi.org/10.1016/S0146-6380(86)80013-4

Whitman W. B., Bowen T. L., & Boone D. R. (2006) The methanogenic bacteria, in The Prokaryotes, Dworkin M.; Falkow S.; Rosenberb E.; Schleifer K.; Stackebrandt, E., EDs. Springer: New York, NY, 2006; Vol. 3, pp 165-207.

Williams, A. G., & Scherer, M. M. (2004). Spectroscopic evidence for Fe(II)-Fe(III) electron transfer at the iron oxide-water interface. Environmental Science and Technology, 38(18), 4782-4790. https://doi.org/10.1021/es049373g

Appendix A - Ferric Iron Mineral Experiments

Sample name	Ferric iron mineral	Live/ sterile	Acetate (mM)	pH	Fe(II) (0.5 N HCl) (µmol)	Fe(II) (aqueous) (µmol)	G. *metallire ducens* cell count	*M. barkeri* cell count
N30A	None	Live	30	7.15	-	-	2.34E+06	1.06E+05
N30B	None	Live	30	7.12	-	-	1.77E+06	8.27E+04
N30C	None	Live	30	6.97	-	-	1.71E+06	9.74E+04
N30S	None	Sterile	30	6.91	-	-	4.59E+05	0.00E+00
N3A	None	Live	3	6.94	-	-	1.43E+06	1.18E+04
N3B	None	Live	3	6.95	-	-	9.52E+05	1.18E+04
N3C	None	Live	3	6.95	-	-	6.73E+05	2.95E+04
N3S	None	Sterile	3	6.92	-	-	2.95E+04	5.90E+03
G30A	Goethite	Live	30	7.18	226.2	3.5	3.67E+06	1.06E+05
G30B	Goethite	Live	30	7.13	233.2	11.6	3.66E+06	5.90E+04
G30C	Goethite	Live	30	7.02	264.5	13.8	2.98E+06	3.84E+04
G30S	Goethite	Sterile	30	6.97	80.1	5.5	5.09E+05	0.00E+00
G3A	Goethite	Live	3	7.08	280.9	2.4	3.51E+06	2.66E+04
G3B	Goethite	Live	3	7.09	236.6	2.1	2.85E+06	1.18E+04
G3C	Goethite	Live	3	6.99	249.6	5.5	3.48E+06	1.18E+04
G3S	Goethite	Sterile	3	6.96	77.2	4.8	8.81E+05	0.00E+00
F30A	Ferrihydrite	Live	30	7.33	314.5	2.5	2.59E+06	1.98E+05
F30B	Ferrihydrite	Live	30	7.19	183.5	8.9	1.21E+05	4.13E+04
F30C	Ferrihydrite	Live	30	7.15	195.4	4.7	1.55E+06	0.00E+00
F30S	Ferrihydrite	Sterile	30	7.09	169.3	8.4	1.18E+04	0.00E+00
F3A	Ferrihydrite	Live	3	7.12	296.0	8.0	6.35E+04	5.90E+03
F3B	Ferrihydrite	Live	3	7.15	253.4	9.6	1.20E+05	2.95E+04
F3C	Ferrihydrite	Live	3	7.22	200.3	5.3	1.03E+05	5.90E+03
F3S	Ferrihydrite	Sterile	3	7.16	183.5	5.6	7.53E+04	0.00E+00
L30A	Lepidocrocite	Live	30	7.16	175.7	22.4	3.64E+06	5.90E+03
L30B	Lepidocrocite	Live	30	7.19	238.0	28.1	3.33E+06	0.00E+00
L30C	Lepidocrocite	Live	30	7.25	200.4	43.9	2.39E+06	0.00E+00
L30S	Lepidocrocite	Sterile	30	6.93	102.1	8.6	4.58E+04	0.00E+00
L3A	Lepidocrocite	Live	3	7.21	242.4	27.4	3.55E+06	0.00E+00
L3B	Lepidocrocite	Live	3	7.28	185.9	30.4	3.87E+06	0.00E+00
L3C	Lepidocrocite	Live	3	7.27	204.7	41.2	2.35E+06	0.00E+00
L3S	Lepidocrocite	Sterile	3	6.96	91.9	10.5	8.12E+04	0.00E+00
H30A	Hematite	Live	30	7.21	159.5	4.4	1.04E+06	9.45E+04
H30B	Hematite	Live	30	7.24	161.9	8.0	4.35E+05	2.95E+04
H30C	Hematite	Live	30	7.28	118.0	0.5	2.06E+06	1.56E+06
H30S	Hematite	Sterile	30	7.00	51.4	7.3	1.33E+04	0.00E+00
H3A	Hematite	Live	3	7.01	129.0	5.7	3.25E+04	8.86E+03
H3B	Hematite	Live	3	7.07	135.7	4.3	1.52E+06	2.07E+04

Sample name	Ferric iron mineral	Live/ sterile	Acetate (mM)	pH	Fe(II) (0.5 N HCl) (µmol)	Fe(II) (aqueous) (µmol)	G. *metallire ducens* cell count	*M. barkeri* cell count
H3C	Hematite	Live	3	7.01	138.3	8.6	1.73E+05	5.90E+03
H3S	Hematite	Sterile	3	6.98	45.6	7.4	2.95E+04	2.95E+03

Sample name	Total pressure (kPa)	$\%CH_4$ (gas)	CH_4 partial pressure (kPa)	CH_4 total (µmol)	$\Delta^{13}C$	Alkalinity (meq/l)	$\%CO_2$	CO_2 partial pressure (kPa)
N30A	132.4	30.75	40.7	946.5	31.7	52.1	12.6	16.7
N30B	142.7	30.0	42.8	995.5	33.1	-	12.5	17.8
N30C	142.7	15.4	21.9	509.4	39.3	-	13.8	19.7
N30S	118.6	0.0	-	0.6	-	40.9	15.9	18.8
N3A	116.8	3.8	4.4	102.3	41.8	30.9	16.2	18.9
N3B	116.8	3.0	3.6	82.6	43.0	-	16.5	19.3
N3C	115.1	1.4	1.6	36.9	44.7	-	16.8	19.3
N3S	111.7	0.0	-	0.3	-	29.9	16.4	18.4
G30A	149.6	22.4	33.9	787.9	38.9	51.5	13.0	19.4
G30B	156.5	31.0	48.4	1126.3	36.2	-	12.2	19.1
G30C	127.2	9.8	12.4	288.4	-	-	14.8	18.8
G30S	115.1	0.0	-	0.5	-	46.8	16.0	18.4
G3A	109.9	0.2	0.2	4.6	35.7	26.4	16.9	18.5
G3B	113.4	0.2	0.2	5.6	36.5	-	17.0	19.2
G3C	111.7	0.2	0.2	5.1	36	-	17.2	19.2
G3S	109.9	0.0	-	0.1	-	28.5	17.1	18.7
F30A	151.3	28.7	43.4	10008.1	37.1	55.4	10.3	15.5
F30B	111.7	0.6	0.7	15.7	44.7	-	11.9	13.3
F30C	111.7	0.0	0.0	0.3	-	-	12.9	14.3
F30S	120.3	0.0	-	0.2	-	46.8	14.0	16.8
F3A	108.2	0.0	0.0	0.2	-	31.1	13.3	14.4
F3B	108.2	0.0	0.0	0.2	-	-	12.8	13.9
F3C	108.2	0.0	0.0	0.2	-	-	13.2	14.3
F3S	108.2	0.0	-	0.1	-	29.5	12.6	13.6
L30A	111.7	2.4	2.7	63.4	45.6	47.0	11.2	12.5
L30B	120.3	7.5	9.0	208.4	43.3	-	10.9	13.1
L30C	108.2	0.4	0.5	11.1	46.4	-	10.3	11.1
L30S	115.1	0.0	-	0.1	-	46.7	16.8	19.3
L3A	122.0	0.2	0.2	4.6	46.3	31.5	11.6	14.1
L3B	101.3	0.0	0.0	0.2	-	-	10.3	10.4
L3C	104.8	0.0	0.0	0.1	-	-	10.0	10.4
L3S	115.1	0.0	-	0.1	-	28.3	16.0	18.4
H30A	194.4	44.6	86.6	2014.1	27.4	51.9	9.8	19.1
H30B	203.0	47.0	95.3	2216.7	24.7	-	9.4	19.0

Sample name	Total pressure (kPa)	%CH_4 (headspace gas)	CH_4 partial pressure (kPa)	CH_4 total (µmol)	$\Delta^{13}C$	Alkalinity (meq/l)	%CO_2	CO_2 partial pressure (kPa)
H30C	197.9	41.8	82.6	1921.0	25	-	9.4	18.5
H30S	116.8	0.1	-	2.5	-	41.1	15.9	18.6
H3A	123.7	9.1	11.3	261.8	31	32.2	15.4	19.0
H3B	120.3	6.2	7.4	172.0	37.4	-	15.9	19.1
H3C	125.5	10.1	12.6	293.2	28.6	-	15.7	19.7
H3S	113.4	0.0	-	1.3	-	28.6	16.4	18.5

Sample name	Cl^- (mg/l)	Br^- (mg/l)	NO_3^- (mg/l)	SO_4^{2-} (mg/l)	Na^+ (mg/l)	K^+ (mg/l)	Mg^{2+} (mg/l)	Ca^{2+} (mg/l)
N30A	1928.59	n.a.	0.8928	6.780	1964.04	201.28	10.59	36.45
N30B	1890.94	n.a.	0.7478	7.149	1985.26	185.77	26.57	29.26
N30C	1940.60	0.0795	0.9536	6.148	1888.46	197.88	30.19	37.08
N30S	1916.61	0.1124	7.9579	4.660	2047.58	208.19	28.47	32.41
N3A	1980.94	0.0841	8.0623	6.600	1488.42	209.61	27.88	23.98
N3B	1982.42	0.1085	8.3094	6.151	1496.28	213.91	27.00	27.49
N3C	2032.23	0.0887	12.1392	6.431	1472.72	206.76	32.17	26.65
N3S	1942.03	0.1564	11.3053	6.078	1475.70	210.85	37.03	34.32
G30A	1918.03	0.0490	0.7478	7.603	1937.10	221.10	31.22	34.08
G30B	1831.10	n.a.	0.6172	7.292	1988.38	228.20	45.88	52.42
G30C	1866.51	0.0727	0.8157	7.294	1986.26	226.84	45.32	16.92
G30S	1926.04	0.0997	0.9289	6.996	1936.82	224.48	41.92	48.44
G3A	2007.87	0.1324	1.0817	7.713	1381.00	229.97	39.73	45.24
G3B	1896.32	0.0943	0.9733	7.421	1484.64	230.79	48.45	58.28
G3C	1880.34	0.0748	0.8113	7.674	1554.40	226.06	46.85	55.52
G3S	2027.07	0.1116	1.0222	7.219	1464.81	236.90	40.93	41.81
F30A	2001.58	n.a.	5.0403	4.324	1941.62	200.42	25.60	17.95
F30B	1750.76	0.1015	1.0179	4.472	1951.23	198.09	29.40	22.71
F30C	1604.69	0.1096	1.0816	4.354	1977.50	200.84	29.66	23.89
F30S	1716.50	0.0932	0.9884	4.385	1975.14	196.77	29.00	35.54
F3A	1878.22	0.0816	0.9294	4.666	1463.55	206.61	25.56	17.88
F3B	1992.16	0.0935	1.0388	4.785	1503.02	211.21	31.74	30.99
F3C	1989.24	0.0778	0.9160	4.826	1482.79	210.33	26.81	32.26
F3S	2001.73	0.0736	0.9816	4.654	1464.84	210.53	28.34	24.31
L30A	1911.77	0.0947	0.8586	4.776	1991.00	223.02	30.07	41.93
L30B	1861.24	0.0736	0.8043	4.747	1931.26	223.80	34.13	57.44
L30C	2003.81	0.0764	0.7666	4.887	1936.33	225.17	39.06	68.99
L30S	1855.00	0.1109	0.932	4.643	2003.84	224.80	37.35	51.16
L3A	1972.99	0.0696	0.8171	4.985	1460.40	204.82	16.05	21.91
L3B	1998.60	0.0796	0.8783	5.055	1350.05	197.27	18.51	32.79

Sample name	Cl^- (mg/l)	Br^- (mg/l)	NO_3^- (mg/l)	SO_4^{2-} (mg/l)	Na^+ (mg/l)	K^+ (mg/l)	Mg^{2+} (mg/l)	Ca^{2+} (mg/l)
L3C	1963.47	0.0841	0.9022	5.092	1450.99	201.83	15.04	18.30
L3S	2030.23	0.1144	1.0519	4.706	1519.68	213.14	22.20	22.78
H30A	1912.98	n.a.	3.8471	6.826	1908.31	195.20	18.88	16.54
H30B	1910.22	n.a.	1.4151	6.610	1919.70	207.82	20.12	16.07
H30C	1881.35	n.a.	0.4717	6.632	1791.50	194.86	19.68	26.18
H30S	1903.42	0.1231	8.4853	5.723	1903.27	196.84	21.88	16.80
H3A	1912.98	0.0812	8.1254	6.892	1481.94	205.76	19.74	17.85
H3B	1910.22	0.0932	1.0906	6.824	1405.87	209.70	21.86	23.56
H3C	1881.35	0.0873	1.0477	7.087	1450.74	205.15	22.67	33.86
H3S	1903.42	0.1251	8.1029	5.915	1481.14	212.07	23.34	18.50

P values from T tests	L3A µmol CH_4 produced	L30A µmol CH_4 produced	G3A µmol CH_4 produced	G30A µmol CH_4 produced	F3A µmol CH_4 produced	F30A µmol CH_4 produced	H3A µmol CH_4 produced	H30A µmol CH_4 produced	N3A µmol CH_4 produced	N30A µmol CH_4 produced
L3A µmol CH_4 produced	1	0.1916	0.0849	0.0396	0.3817	0.3658	0.0027	<0.0001	0.0204	0.0062
L30A µmol CH_4 produced	0.1916	1	0.2051	0.0630	0.1860	0.5060	0.0994	<0.0001	0.7596	0.0120
G3A µmol CH_4 produced	0.0849	0.2051	1	0.0401	<0.0001	0.3702	0.0028	<0.0001	0.0236	0.0063
G30A µmol CH_4 produced	0.0396	0.0630	0.0401	1	0.0393	0.3952	0.1163	0.0070	0.0539	0.7879
F3A µmol CH_4 produced	0.3817	0.1860	<0.0001	0.0393	1	0.3640	0.0026	<0.0001	0.0189	0.0061
F30A µmol CH_4 produced	0.3658	0.5060	0.3702	0.3952	0.3640	1	0.7825	0.0077	0.4681	0.2651
H3A µmol CH_4 produced	0.0027	0.0994	0.0028	0.1163	0.0026	0.7825	1	<0.0001	0.0149	0.0223
H30A µmol CH_4 produced	<0.0001	<0.0001	<0.0001	0.0070	<0.0001	0.0077	<0.0001	1	<0.0001	0.0023
N3A µmol CH_4 produced	0.0204	0.7596	0.0236	0.0539	0.0189	0.4681	0.0149	<0.0001	1	0.0088
N30A µmol CH_4 produced	0.0062	0.0120	0.0063	0.7879	0.0061	0.2651	0.0223	0.0023	0.0088	1

P values from T tests	L3A µmol 0.5 N HCl Fe(II)	L30A µmol 0.5 N HCl Fe(II)	G3A µmol 0.5 N HCl Fe(II)	G30A µmol 0.5 N HCl Fe(II)	F3A µmol 0.5 N HCl Fe(II)	F30A µmol 0.5 N HCl Fe(II)	N3A µmol 0.5 N HCl Fe(II)	N30A µmol 0.5 N HCl Fe(II)
L3A µmol 0.5 N HCl Fe(II)	1	0.8103	0.1025	0.2109	0.2946	0.6778	0.0104	0.0420
L30A µmol 0.5 N HCl Fe(II)	0.8103	1	0.0849	0.1655	0.2436	0.5930	0.0185	0.0649
G3A µmol 0.5 N HCl Fe(II)	0.1025	0.0849	1	0.4603	0.8591	0.6051	0.0008	0.0049
G30A µmol 0.5 N HCl Fe(II)	0.2109	0.1655	0.4603	1	0.7892	0.8265	0.0009	0.0068
F3A µmol 0.5 N HCl Fe(II)	0.2946	0.2436	0.8591	0.7892	1	0.7273	0.0142	0.0293
F30A µmol 0.5 N HCl Fe(II)	0.6778	0.5930	0.6051	0.8265	0.7273	1	0.0821	0.0649
N3A µmol 0.5 N HCl Fe(II)	0.0104	0.0185	0.0008	0.0009	0.0142	0.0821	1	0.4503
N30A µmol 0.5 N HCl Fe(II)	0.0420	0.0649	0.0049	0.0068	0.0293	0.0649	0.4503	1

Appendix B - Semi-Continuous Experiments

Sample name	Live/sterile	HCO_3^- (mM)	Acetate (mM)
24-30-A	Live	24	30
24-30-B	Live	24	30
24-30-C	Live	24	30
24-30-S	Sterile	24	30
24-3-A	Live	24	3
24-3-B	Live	24	3
24-3-C	Live	24	3
24-3-S	Sterile	24	3
48-30-A	Live	48	30
48-30-B	Live	48	30
48-30-C	Live	48	30
48-30-S	Sterile	48	30
48-3-A	Live	48	3
48-3-B	Live	48	3
48-3-C	Live	48	3
48-3-S	Sterile	48	3

Sample name	7/10/20 pH	7/17/20 pH	7/24/20 pH	7/31/20 pH	8/7/20 pH	8/14/20 pH	8/21/20 pH	8/29/20 pH
24-30-A	7.02	6.91	6.95	6.88	6.96	6.99	6.91	6.90
24-30-B	6.93	6.88	6.94	6.91	6.97	6.96	6.98	7.04
24-30-C	6.92	6.89	6.89	6.89	6.97	6.96	6.94	6.98
24-30-S	7	6.96	9.98	6.92	6.92	7.06	6.90	6.86
24-3-A	6.93	6.89	6.93	6.90	7.00	6.98	6.93	6.91
24-3-B	6.98	6.89	6.98	6.94	6.95	6.91	6.89	6.89
24-3-C	6.91	6.89	6.94	6.89	6.99	6.93	6.91	6.89
24-3-S	6.97	6.94	6.97	6.94	6.97	7.01	6.95	6.89
48-30-A	7.13	7.26	7.28	7.06	7.16	7.09	7.06	7.13
48-30-B	7.15	7.21	7.38	7.26	7.12	7.26	7.07	7.13
48-30-C	7.12	7.09	7.09	7.02	7.08	7.04	7.06	7.12
48-30-S	7.12	7.12	7.12	7.12	7.15	7.17	7.04	7.02
48-3-A	7.16	7.14	7.10	7.14	7.14	7.11	7.09	7.05
48-3-B	7.14	7.12	7.11	7.11	7.14	7.07	7.04	7.09
48-3-C	7.12	7.09	7.08	7.14	7.09	7.05	7.03	7.00
48-3-S	7.14	7.10	7.08	7.22	7.15	7.05	7.05	7.04

Sample name	7/10/20 G. *metallireducens* cell count	8/7/20 G. *metallireducens* cell count	8/21/20 G. *metallireducens* cell count	7/10/20 *M. barkeri* cell count	8/7/20 *M. barkeri* cell count	8/21/20 *M. barkeri* cell count
24-30-A	4.03E+06	2.28E+05	3.09E+06	7.77E+04	5.09E+0	1.76E+06
24-30-S	1.53E+05	8.71E+04	9.60E+04	2.95E+03	7.32E+05	7.38E+03
24-3-A	4.57E+06	2.46E+06	4.01E+06	3.25E+04	1.05E+06	1.13E+04
24-3-S	2.10E+05	1.20E+06	7.23E+04	1.30E+05	6.14E+05	0.00E+00
48-30-A	4.72E+06	2.92E+06	1.95E+06	9.00E+04	1.62E+04	1.29E+04
48-30-S	2.21E+05	2.45E+06	3.54E+04	1.09E+05	9.30E+04	0.00E+00
48-3-A	4.40E+06	2.33E+06	1.55E+06	1.65E+05	1.48E+04	1.63E+04
48-3-S	1.36E+05	8.38E+05	2.14E+04	6.82E+05	1.62E+04	4.43E+03

Sample name	7/24/20 $\%CH_4$ (headspace gas)	7/24/20 CH_4 partial pressure (kPa)	7/24/20 CH_4 total (µmol)	7/24/20 $\Delta^{13}C$	7/24/20 $\%CO_2$	7/24/20 CO_2 partial pressure (kPa)
24-30-A	.56	0.6	14.4	38.1	17.4	20.0
24-30-B	-	-	-	-	-	-
24-30-C	-	-	-	-	-	-
24-30-S	0.0	0.0	0.0	-	17.1	17.3
24-3-A	0.6	0.6	13.6	32.9	17.6	19.0
24-3-B	0.1	0.1	2.3	32.9	16.3	16.5
24-3-C	0.0	0.0	1.1	35.1	17.6	17.8
24-3-S	0.1	0.1	1.2	-	17.3	17.5
48-30-A	0.3	7.8	7.8	30.1	21.4	21.6
48-30-B	0.4	8.6	8.6	30.5	21.6	22.6
48-30-C	0.7	16.6	16.6	31.5	22.2	24.0
48-30-S	0.0	0.1	0.1	-	18.8	20.3
48-3-A	0.1	2.1	2.1	30.4	23.1	23.4
48-3-B	0.0	1.3	1.3	33.3	21.5	24.8
48-3-C	0.1	1.9	1.9	31.2	23.0	24.8
48-3-S	0.0	0.6	0.6	-	24.0	24.3

Sample name	8/7/20 %CH_4 (headspace gas)	8/7/20 CH_4 partial pressure (kPa)	8/7/20 CH_4 total (µmol)	8/7/20 $\Delta^{13}C$	8/7/20 %CO_2	8/7/20 CO_2 partial pressure (kPa)
24-30-A	3.0	3.3	75.8	31.7	16.6	18.2
24-30-B	8.0	9.2	214.2	32.8	16.4	18.8
24-30-C	7.3	8.4	195.4	33.3	17.0	19.5
24-30-S	0.0	0.0	0.1	-	18.2	18.4
24-3-A	0.5	0.6	13.0	35.4	17.8	19.3
24-3-B	0.5	0.5	11.9	35.6	18.1	19.5
24-3-C	0.3	0.3	7.9	35.1	28.9	29.2
24-3-S	-	-	-	-	17.6	17.8
48-30-A	2.7	3.0	69.2	29.8	23.7	26.4
48-30-B	2.0	2.3	52.5	30.2	23.8	26.5
48-30-C	6.1	7.0	163.3	24.4	21.4	24.6
48-30-S	0.0	0.0	0.1	-	24.4	24.7
48-3-A	0.3	0.3	7.5	32.7	27.1	29.3
48-3-B	0.2	0.2	5.7	31.6	17.1	19.6
48-3-C	0.4	0.5	11.1	33.5	26.5	28.6
48-3-S	0.0	0.0	0.0	-	21.1	22.1

Sample name	8/29/20 %CH_4 (headspace gas)	8/29/20 CH_4 partial pressure (kPa)	8/29/20 CH_4 total (µmol)	8/29/20 $\Delta^{13}C$	8/29/20 %CO_2	8/29/20 CO_2 partial pressure (kPa)
24-30-A	4.1	4.7	108.8	32.4	11.5	13.2
24-30-B	32.9	50.8	1182.3	27	11.8	18.2
24-30-C	28.1	40.0	930.8	27.9	13,1	18.7
24-30-S	0.0	0.0	0.6	-	14.2	14.8
24-3-A	1.0	1.1	25.9	32.9	14.1	15.3
24-3-B	0.9	1.0	23.4	33.3	12.6	13.6
24-3-C	0.9	1.0	22.9	31.0	13.7	14.8
24-3-S	0.0	0.0	0.0	-	13.1	13.3
48-30-A	4.0	4.5	105.7	30.1	22.4	25.7
48-30-B	2.4	2.7	62.8	29.7	22.6	25.6
48-30-C	-	-	-	-	-	-
48-30-S	0.0	0.0	0.2	-	23.0	24.8
48-3-A	0.4	0.4	9.6	34.1	25.5	27.6
48-3-B	0.5	0.6	13.2	32.0	23.9	27.5
48-3-C	0.6	0.7	16.0	32.0	24.1	29.3
48-3-S	-	-	-	-	-	-

Sample name	7/17/20 Alkalinity (meq/l)	7/31/20 Alkalinity (meq/l)	8/14/20 Alkalinity (meq/l)	8/29/20 Alkalinity (meq/l)
24-30-A	53.3	50.8	49.2	52.3
24-30-B	39.5	49.5	49.0	52.2
24-30-C	40.0	49.7	46.4	51.7
24-30-S	40.0	46.8	46.8	49.7
24-3-A	28.0	28.8	30.9	28.2
24-3-B	30.4	51.4	30.9	27.4
24-3-C	27.9	28.6	29.2	30.3
24-3-S	27.5	28.3	29.3	28.9
48-30-A	60.7	71.7	80.7	72.4
48-30-B	60.0	73.4	71.5	72.3
48-30-C	60.5	70.6	66.4	72.2
48-30-S	62.9	71.0	71.8	72.3
48-3-A	50.0	52.8	54.0	52.3
48-3-B	50.1	51.4	52.7	52.2
48-3-C	50.1	51.8	53.0	52.6
48-3-S	49.8	50.9	52.9	52.2

P values from T tests	24-3 µmol CH_4 at 21 days	24-30 µmol CH_4 at 21 days	48-3 µmol CH_4 at 21 days	48-30 µmol CH_4 at 21 days	24-3 µmol CH_4 at 35 days	24-30 µmol CH_4 at 35 days	48-3 µmol CH_4 at 35 days	48-30 µmol CH_4 at 35 days	24-3 µmol CH_4 at 56 days	24-30 µmol CH_4 at 56 days	48-3 µmol CH_4 at 56 days	48-30 µmol CH_4 at 56 days
24-3 µmol CH_4 at 21 days	1	0.0020	0.7782	0.0015	0.4609	0.0761	0.1274	0.1621	0.0049	0.1803	0.9470	0.0799
24-30 µmol CH_4 at 21 days	0.0020	1	0.0251	0.9659	0.0048	0.0210	0.0181	0.0539	<0.0001	0.0848	0.0043	0.0142
48-3 µmol CH_4 at 21 days	0.7782	0.0251	1	0.0247	0.8356	0.0259	0.3343	0.0736	0.0134	0.0877	0.7124	0.0215
48-30 µmol CH_4 at 21 days	0.0015	0.9659	0.0247	1	0.0044	0.0210	0.0170	0.0540	<0.0001	0.0848	0.0041	0.0142
24-3 µmol CH_4 at 35 days	0.4609	0.0048	0.8356	0.0044	1	0.0254	0.2729	0.0716	0.0019	0.0875	0.4484	0.0200
24-30 µmol CH_4 at 35 days	0.0761	0.0210	0.0259	0.0210	0.0254	1	0.0239	0.2942	0.0336	0.1514	0.0265	0.2748
48-3 µmol CH_4 at 35 days	0.1274	0.0181	0.3343	0.0170	0.2729	0.0239	1	0.0656	0.0010	0.0867	0.1183	0.0181
48-30 µmol CH_4 at 35 days	0.1621	0.0539	0.0736	0.0540	0.0716	0.2942	0.0656	1	0.1091	0.1187	0.0764	0.8351
24-3 µmol CH_4 at 56 days	0.0049	<0.0001	0.0134	<0.0001	0.0019	0.0336	0.0010	0.1091	1	0.0916	0.0059	0.0332
24-30 µmol CH_4 at 56 days	0.1803	0.0848	0.0877	0.0848	0.0875	0.1514	0.0867	0.1187	0.0916	1	0.0881	0.2150
48-3 µmol CH_4 at 56 days	0.9470	0.0043	0.7124	0.0041	0.4484	0.0265	0.1183	0.0764	0.0059	0.0881	1	0.0217
48-30 µmol CH_4 at 56 days	0.0799	0.0142	0.0215	0.0142	0.0200	0.2748	0.0181	0.8351	0.0332	0.2150	0.0217	1

Appendix C - Methanogen Substrate Experiments

Sample name	Live/sterile	Substrate	Total pressure (kPa)	%CH_4 (headspace gas)	CH_4 partial pressure (kPa)	CH_4 total (μmol)	$\Delta^{13}C$	%CO_2	CO_2 partial pressure (kPa)
HA	Live	H_2	101.3	5.3	5.4	124.9	33.6	15.8	16.0
HB	Live	H_2	101.3	4.7	4.8	111.5	32.3	15.6	15.8
HC	Live	H_2	101.3	4.1	4.2	97.0	32.1	12.9	13.0
HS	Sterile	H_2	109.9	-	-	-	-	-	-
MA	Live	Methanol	159.9	29.4	47.0	1093.5	31.9	15.5	24.7
MB	Live	Methanol	161.7	29.3	47,4	1101.5	31.3	15.8	25.5
MC	Live	Methanol	156.5	-	-	-	-	-	-
MS	Sterile	Methanol	111.7	-	-	-	-	-	-
AA	Live	Acetate	203.0	48.2	97,9	2275.7	22.2	9.8	19.9
AB	Live	Acetate	218.5	54.5	119.1	2769.8	18.3	9.1	19.8
AC	Live	Acetate	209.9	50.25	105.5	2453.1	23.2	9.3	19.4
AS	Sterile	Acetate	115.1	0.0	-	0.0	26.7	15.8	18.1

P values from T tests	H_2 substrate $\Delta^{13}C$	Acetate substrate $\Delta^{13}C$
H_2 substrate $\Delta^{13}C$	1	0.0019
Acetate substrate $\Delta^{13}C$	0.0019	1
24-3 $\Delta^{13}C$ at 21 days	0.3294	0.0017
24-30 $\Delta^{13}C$ at 21 days	0.0287	0.0300
48-3 $\Delta^{13}C$ at 21 days	0.3531	0.0038
48-30 $\Delta^{13}C$ at 21 days	0.0351	0.0037
24-3 $\Delta^{13}C$ at 35 days	0.0054	0.0007
24-30 $\Delta^{13}C$ at 35 days	0.9252	0.0019
48-3 $\Delta^{13}C$ at 35 days	0.9311	0.0020
48-30 $\Delta^{13}C$ at 35 days	0.0784	0.0449
24-3 $\Delta^{13}C$ at 56 days	0.7697	0.0025
24-30 $\Delta^{13}C$ at 56 days	0.1090	0.0247
48-3 $\Delta^{13}C$ at 56 days	0.9704	0.0023
48-30 $\Delta^{13}C$ at 56 days	0.0214	0.0208
L3 $\Delta^{13}C$	0.0047	0.0139
L30 $\Delta^{13}C$	0.0003	0.0002
G3 $\Delta^{13}C$	0.0029	0.0006
G30 $\Delta^{13}C$	0.0253	0.0049
F3 $\Delta^{13}C$	No data	No data
F30 $\Delta^{13}C$	0.0655	0.0105
H3 $\Delta^{13}C$	0.9066	0.0213
H30 $\Delta^{13}C$	0.0020	0.0604
N3 $\Delta^{13}C$	0.0004	0.0002
N30 $\Delta^{13}C$	0.4414	0.0083